

**On the exploration of regression dependence structures
in multidimensional contingency tables with ordinal response variables**

Zheng Wei, Li Wang, Shu-Min Liao, Daeyoung Kim

Texas A&M University-Corpus Christi, Microsoft,

Amherst College and University of Massachusetts-Amherst

Supplementary Material

The supplementary material presents the simulation studies to examine (i) the finite-sample performance of the estimators of the proposed Scaled CCRAM (SCCRAM)s and (ii) the sizes and powers of the permutation tests associated with the SCCRAMs which are summarized in the Discussion section of the main article.

S1. Simulation for finite-sample properties of the estimators of the SCCRAMs

S1.1. Design of simulation study

We design a simulation study to evaluate the performance of the estimators of the proposed Scaled CCRAM (SCCRAM)s in a three-way ordinal contingency table with the ordinal response variable Y and two ordinal independent variables X_1 and X_2 . Since the sequential decomposition of $\rho_{(X_1, X_2 \rightarrow Y)}^{2*}$ under a three-way ordinal contingency table is given by

$$\rho_{(X_1, X_2 \rightarrow Y)}^{2*} = \rho_{(X_1 \rightarrow Y)}^{2*} + \rho_{(X_2 \rightarrow Y|X_1)}^{2*} = \rho_{(X_2 \rightarrow Y)}^{2*} + \rho_{(X_1 \rightarrow Y|X_2)}^{2*},$$

thus, we can consider the five SCCRAMs : an overall SCCRAM $\rho^2_{(X_1, X_2 \rightarrow Y)}$, two marginal SCCRAMs, $\rho^2_{(X_1 \rightarrow Y)}$ and $\rho^2_{(X_2 \rightarrow Y)}$, and two conditional SCCRAMs, $\rho^2_{(X_2 \rightarrow Y|X_1)}$ and $\rho^2_{(X_1 \rightarrow Y|X_2)}$.

For the simulation study, the following three simulation factors are considered : (i) table size (number of categories of Y , X_1 and X_2 , denoted as J , I_1 and I_2 , respectively), (ii) total sample size n , and (iii) magnitude of marginal and conditional associations between Y and X_1 , unconditional and conditional on X_2 , $\rho^2_{(X_1 \rightarrow Y)}$ and $\rho^2_{(X_1 \rightarrow Y|X_2)}$, respectively.

For the table size, we consider a three-way square contingency table whose size is $3 \times 3 \times 3$, $5 \times 5 \times 5$ and $7 \times 7 \times 7$ (i.e., three values of $(J, I_1, I_2) = (3, 3, 3), (5, 5, 5), (7, 7, 7)$). To adequately assess the effect of the total sample size (n), we manipulate six levels of cell frequency (n_c) from small, to medium to large, that is $n_c = (5, 10, 20, 40, 80, 160)$, and then obtain the total sample size n by taking into account the number of categories of each variable, $n = n_c \times J \times I_1 \times I_2$: $n = (135, 270, 540, 1080, 2160, 4320)$ for $J = I_1 = I_2 = 3$ ($3 \times 3 \times 3$ table), $n = (625, 1250, 2500, 5000, 10000, 20000)$ for $J = I_1 = I_2 = 5$ ($5 \times 5 \times 5$ table), and $n = (1715, 3430, 6860, 13720, 27440, 54880)$ for $J = I_1 = I_2 = 7$ ($7 \times 7 \times 7$ table). Note that standard asymptotic theory under a multinomial sampling scheme assumes that a number of categories of the variables is fixed while the cell expected frequencies go to infinity [1].

To generate a three-way ordinal contingency table giving the frequencies of n observations cross-classified by three ordinal variables (Y, X_1, X_2) , we use a latent variable approach which assumes that a trivariate standard normal distribution with three pairwise correlations underlies three ordinal variables in the three-way contingency table. This can be done using the function `ordsample` in the R package, `GenOrd` [2], whose basic idea is to transform multivariate normal

variables with a given correlation matrix into multivariate ordinal variables with the desired correlation matrix and marginal distributions. For the details, please refer to [3]. The third simulation factor, the magnitude of marginal and conditional associations between Y and X_1 unconditional and conditional on X_2 , is determined by the marginal distributions of three ordinal variables and their target correlation matrix consisting of three pairwise correlations, denoted as r_{YX_1} between Y and X_1 , r_{YX_2} between Y and X_2 , and $r_{X_1X_2}$ between X_1 and X_2 . We consider the four sets of $(r_{YX_1}, r_{YX_2}, r_{X_1X_2})$, denoted as I, II, III, and IV, as shown in Table S1. While r_{YX_2} is fixed to be 0.4, $r_{X_1X_2}$ increases from zero to 0.25 to 0.5 to 0.75 throughout the four sets I-IV. Within each set, the four values of r_{YX_1} were chosen to represent different degree of correlation between Y and X_1 . That is, (0, 0.229, 0.458, 0.687) for set I (denoted as I-1 ~ I-4), (0.1, 0.322, 0.544, 0.766) for set II (denoted as II-1 ~ II-4), (0.2, 0.3985, 0.597, 0.795) for set III (denoted as III-1 ~ III-4), and (0.3, 0.4515, 0.603, 0.7545) for set IV (denoted as IV-1 ~ IV-4). Furthermore, the marginal distribution for each of three ordinal variables was specified as a discrete uniform distribution. Table S1 presents 16 true values of $(r_{YX_1}, r_{YX_2}, r_{X_1X_2})$ for the four sets I - IV (four cases for each set).

For each case of each set in Table S1, we first construct the three sets of three way *population ordinal contingency table*, $3 \times 3 \times 3$, $5 \times 5 \times 5$ and $7 \times 7 \times 7$ tables. What we mean by the population ordinal contingency table is the contingency table of the population size $N=10^7$ generated by the R function `ordsample` based on three pairwise correlations $(r_{YX_1}, r_{YX_2}, r_{X_1X_2})$ given in Table S1 and the discrete uniform marginals. We then compute the population/true values of the overall/marginal/conditional SCCRAMs for each population contingency table which

are presented in Table S1, denoted as $\rho_{0(X_1, X_2 \rightarrow Y)}^{2*}$, $\rho_{0(X_1 \rightarrow Y)}^{2*}$, $\rho_{0(X_2 \rightarrow Y|X_1)}^{2*}$, $\rho_{0(X_2 \rightarrow Y)}^{2*}$ and $\rho_{0(X_1 \rightarrow Y|X_2)}^{2*}$. The population values of the five SCCRAMs show various patterns of overall/marginal/conditional association. That is, $\rho_{0(X_1, X_2 \rightarrow Y)}^{2*}$ gradually increases from around 0.16 to around 0.63-0.64. The values of $\rho_{0(X_1 \rightarrow Y)}^{2*}$ and $\rho_{0(X_1 \rightarrow Y|X_2)}^{2*}$ increase starting from 0 or the neighborhood of 0, while $\rho_{0(X_2 \rightarrow Y)}^{2*}$ is constant around 0.16 and $\rho_{0(X_2 \rightarrow Y|X_1)}^{2*}$ either stays in the neighborhood of 0 or 0.16 or gradually decreases toward 0.

To sum up, the simulation factors are

- three levels of table size : $3 \times 3 \times 3$, $5 \times 5 \times 5$ and $7 \times 7 \times 7$ ($J = I_1 = I_2 = 3, 5, 7$)
- six levels of the total sample size for each table size : $n = (135, 270, 540, 1080, 2160, 4320)$ for $3 \times 3 \times 3$ table, $n = (625, 1250, 2500, 5000, 10000, 20000)$ for $5 \times 5 \times 5$ table, and $n = (1715, 3430, 6860, 13720, 27440, 54880)$ for $7 \times 7 \times 7$ table from $n = n_c \times J \times I_1 \times I_2$ with $n_c = (5, 10, 20, 40, 80, 160)$
- 16 levels of magnitude of marginal and conditional association between Y and X_1 : four cases 1-4 under each set I-IV in Table S1

For each combination of simulation factors, we simulated 1000 three-way contingency tables of sample size n , and for each simulated contingency table, we then compute the estimates of the five SCCRAMs, denoted as $\hat{\rho}_{0(X_1, X_2 \rightarrow Y)}^{2*}$, $\hat{\rho}_{0(X_1 \rightarrow Y)}^{2*}$, $\hat{\rho}_{0(X_2 \rightarrow Y|X_1)}^{2*}$, $\hat{\rho}_{0(X_2 \rightarrow Y)}^{2*}$ and $\hat{\rho}_{0(X_1 \rightarrow Y|X_2)}^{2*}$.

S1.1 Design of simulation study

Table S1: True values of $(r_{YX_1}, r_{YX_2}, r_{X_1X_2})$ and the corresponding values of SCCRAMs, $\rho_{0(X_1, X_2 \rightarrow Y)}^{2*}, \rho_{0(X_1 \rightarrow Y)}^{2*}, \rho_{0(X_2 \rightarrow Y|X_1)}^{2*}, \rho_{0(X_2 \rightarrow Y)}^{2*}$ and $\rho_{0(X_1 \rightarrow Y|X_2)}^{2*}$ used in the simulation of the performance of the overall, marginal and conditional SCCRAMs

Set	r_{YX_1}	r_{YX_2}	$r_{X_1X_2}$	Table	$\rho_{0(X_1, X_2 \rightarrow Y)}^{2*}$	$\rho_{0(X_1 \rightarrow Y)}^{2*}$	$\rho_{0(X_2 \rightarrow Y X_1)}^{2*}$	$\rho_{0(X_2 \rightarrow Y)}^{2*}$	$\rho_{0(X_1 \rightarrow Y X_2)}^{2*}$
I	1	0	0	$3 \times 3 \times 3$	0.1600	0	0.1600	0.1600	0
				$5 \times 5 \times 5$	0.1611	0	0.1611	0.1611	0
				$7 \times 7 \times 7$	0.1619	0	0.1619	0.1619	0
	2	0.229	0.4	$3 \times 3 \times 3$	0.2128	0.0524	0.1604	0.1600	0.0528
				$5 \times 5 \times 5$	0.2143	0.0529	0.1614	0.1611	0.0532
				$7 \times 7 \times 7$	0.2156	0.0533	0.1622	0.1620	0.0536
	3	0.458	0.4	$3 \times 3 \times 3$	0.3730	0.2097	0.1633	0.1600	0.2130
				$5 \times 5 \times 5$	0.3744	0.2109	0.1635	0.1611	0.2133
				$7 \times 7 \times 7$	0.3762	0.2121	0.1641	0.1620	0.2142
	4	0.687	0.4	$3 \times 3 \times 3$	0.6486	0.4720	0.1765	0.1600	0.4885
				$5 \times 5 \times 5$	0.6444	0.4728	0.1715	0.1610	0.4834
				$7 \times 7 \times 7$	0.6449	0.4739	0.1710	0.1621	0.4828
II	1	0.1	0.4	$3 \times 3 \times 3$	0.1601	0.0100	0.1501	0.1599	0.0001
				$5 \times 5 \times 5$	0.1612	0.0101	0.1511	0.1611	0.0001
				$7 \times 7 \times 7$	0.1620	0.0102	0.1518	0.1619	0.0001
	2	0.322	0.4	$3 \times 3 \times 3$	0.2126	0.1037	0.1088	0.1599	0.0526
				$5 \times 5 \times 5$	0.2138	0.1045	0.1093	0.1611	0.0527
				$7 \times 7 \times 7$	0.2147	0.1052	0.1096	0.1620	0.0528
	3	0.544	0.4	$3 \times 3 \times 3$	0.3707	0.2958	0.0748	0.1599	0.2108
				$5 \times 5 \times 5$	0.3720	0.2971	0.0749	0.1611	0.2109
				$7 \times 7 \times 7$	0.3733	0.2984	0.0750	0.1620	0.2113
	4	0.766	0.4	$3 \times 3 \times 3$	0.6362	0.5868	0.0494	0.1600	0.4762
				$5 \times 5 \times 5$	0.6356	0.5871	0.0486	0.1611	0.4746
				$7 \times 7 \times 7$	0.6365	0.5880	0.0484	0.1621	0.4743
III	1	0.2	0.4	$3 \times 3 \times 3$	0.1605	0.0399	0.1206	0.1599	0.0005
				$5 \times 5 \times 5$	0.1614	0.0403	0.1211	0.1610	0.0004
				$7 \times 7 \times 7$	0.1622	0.0406	0.1216	0.1620	0.0002
	2	0.3985	0.4	$3 \times 3 \times 3$	0.2128	0.1588	0.0540	0.1599	0.0528
				$5 \times 5 \times 5$	0.2137	0.1598	0.0539	0.1610	0.0526
				$7 \times 7 \times 7$	0.2145	0.1608	0.0537	0.1620	0.0525
	3	0.597	0.4	$3 \times 3 \times 3$	0.3702	0.3563	0.0139	0.1599	0.2103
				$5 \times 5 \times 5$	0.3712	0.3575	0.0137	0.1610	0.2101
				$7 \times 7 \times 7$	0.3723	0.3588	0.0135	0.1620	0.2102
	4	0.795	0.4	$3 \times 3 \times 3$	0.6326	0.6321	0.0005	0.1600	0.4726
				$5 \times 5 \times 5$	0.6327	0.6322	0.0005	0.1610	0.4716
				$7 \times 7 \times 7$	0.6333	0.6330	0.0003	0.1621	0.4712
IV	1	0.3	0.4	$3 \times 3 \times 3$	0.1609	0.0899	0.0710	0.1600	0.0009
				$5 \times 5 \times 5$	0.1619	0.0907	0.0712	0.1610	0.0009
				$7 \times 7 \times 7$	0.1626	0.0913	0.0713	0.1620	0.0006
	2	0.4515	0.4	$3 \times 3 \times 3$	0.2134	0.2038	0.0096	0.1599	0.0534
				$5 \times 5 \times 5$	0.2145	0.2050	0.0095	0.1611	0.0534
				$7 \times 7 \times 7$	0.2152	0.2062	0.0091	0.1620	0.0532
	3	0.603	0.4	$3 \times 3 \times 3$	0.3719	0.3635	0.0083	0.1599	0.2120
				$5 \times 5 \times 5$	0.3727	0.3646	0.0080	0.1610	0.2116
				$7 \times 7 \times 7$	0.3738	0.3660	0.0078	0.1621	0.2118
	4	0.7545	0.4	$3 \times 3 \times 3$	0.6412	0.5692	0.0720	0.1600	0.4812
				$5 \times 5 \times 5$	0.6397	0.5698	0.0699	0.1611	0.4787
				$7 \times 7 \times 7$	0.6401	0.5707	0.0694	0.1621	0.4781

S1.2. Simulation results

We here investigate the performance of the estimators of overall/marginal/conditional the SCCRAMs, $\hat{\rho}_{(X_1, X_2 \rightarrow Y)}^{2*}$, $\hat{\rho}_{(X_1 \rightarrow Y)}^{2*}$, $\hat{\rho}_{(X_2 \rightarrow Y|X_1)}^{2*}$, $\hat{\rho}_{(X_2 \rightarrow Y)}^{2*}$, and $\hat{\rho}_{(X_1 \rightarrow Y|X_2)}^{2*}$, in terms of unbiasedness, variability, finite-sample distribution, and empirical convergence rate of the estimators.

In order to examine the finite-sample behavior of the estimators in terms of bias, variability and sampling distribution, we present 1000 estimates for each SCCRAM using the boxplots. The plots of the boxplots for $\hat{\rho}_{(X_1, X_2 \rightarrow Y)}^{2*}$, $\hat{\rho}_{(X_1 \rightarrow Y)}^{2*}$, $\hat{\rho}_{(X_2 \rightarrow Y|X_1)}^{2*}$, $\hat{\rho}_{(X_2 \rightarrow Y)}^{2*}$, and $\hat{\rho}_{(X_1 \rightarrow Y|X_2)}^{2*}$ are presented in

- Figures S1 - S4 for Set I-1 ~ Set I-4,
- Figures S5 - S8 for Set II-1 ~ Set II-4,
- Figures S9 - S12 for Set III-1 ~ Set III-4, and
- Figures S13 - S16 for Set IV-1 ~ Set IV-4.

Each figure includes the five plots, one for each SCCRAM : $\hat{\rho}_{(X_1, X_2 \rightarrow Y)}^{2*}$ (first row), $\hat{\rho}_{(X_1 \rightarrow Y)}^{2*}$ (left in the second row), $\hat{\rho}_{(X_2 \rightarrow Y|X_1)}^{2*}$ (right in the second row), $\hat{\rho}_{(X_2 \rightarrow Y)}^{2*}$ (left in the third row), and $\hat{\rho}_{(X_1 \rightarrow Y|X_2)}^{2*}$ (right in the third row). Each plot in each Figure shows boxplots of the estimates of each SCCRAM for the six sample sizes (represented in terms of the cell counts $n_c=(5,10,20,40,80,160)$) under $3 \times 3 \times 3 \times$ table (**black colored boxplot**), $5 \times 5 \times 5 \times$ table (**blue colored boxplot**) and $7 \times 7 \times 7 \times$ table (**red colored boxplot**). In each boxplot the true value of each SCCRAM is represented by the **green dotted line**, and the mean and the median of 1000 estimators are represented by the diamond and the line inside the box.

From the outputs shown in Figures S1 - S16, we have made several observations. First, the bias of the estimator of each (overall/marginal/conditional) SCCRAM tends to decreases as the

total sample size n increases, regardless of the table size and the magnitude of the marginal and conditional SCCRAMs. It is noteworthy to mention that the rate at which bias is attenuated appears to differ, depending on the true values magnitude of the marginal and conditional SCCRAMs. That is, the bias decreases faster as the true values of the SCCRAMs are away from 0. We also observe that the bias of the estimator for the overall SCCRAM $\rho_{(X_1, X_2 \rightarrow Y)}^{2*}$ appears to be smaller when none of the true values of the marginal and conditional SCCRAMs is close to 0, and the bias of the estimator for the conditional SCCRAM $\rho_{(X_2 \rightarrow Y|X_1)}^{2*}$ seems to be smaller when the corresponding marginal SCCRAM $\rho_{(X_1 \rightarrow Y)}^{2*}$ is away from 0.

Second, the variability of the estimator of each SCCRAM has a tendency to decrease as n increases, regardless of the magnitude of the (marginal/conditional) SCCRAMs and the table size. Third, when the true values for the SCCRAMs are away from 0, the sampling distributions of the corresponding estimators appear to be symmetric, irrespective of the table size and the total sample size. Note when n is smaller ($n_c = 5$), the sampling distributions for the estimators of the marginal and conditional SCCRAMs appear to be slightly skewed right. On the other hand, the sampling distributions of the estimators for $\rho_{(X_1 \rightarrow Y)}^{2*}$ and $\rho_{(X_1 \rightarrow Y|X_2)}^{2*}$ appear to be heavily skewed to the right, especially when the true value is exactly 0 (regardless of n) or when their true values are close to 0 (0.05 and below) and n is small or moderate ($n_c = 5, 10, 20$).

Next, we examine a possible convergence rate of each SCCRAM as the total sample size n tends to infinity for a given true value of the corresponding SCCRAM and table size. To this end, we estimate the empirical convergence rate by the slope of the least-squares linear fit applied to the log-log plot of the RMSE of the 1000 estimates for each SCCRAM and the total

sample size n at each table size, and we then present the results in Table S3. Note that three numbers in the parenthesis for a given parameter set and SCCRAM represent the empirical convergence rates obtained for three table sizes : the first number for $3 \times 3 \times 3$ table, the second number for $5 \times 5 \times 5$ table, and the third number for $7 \times 7 \times 7$ table.

We found that the log-log plot of the RMSE shows a downward linear pattern with slope of approximately -0.5 or -1, depending on the true value of the SCCRAM only. When the true values of the SCCRAMs are away from 0, then the slopes tend to be approximately -0.5. It indicates that the empirical convergence rates of the estimators are approximately of order $n^{-0.5}$, which is the rate of convergence for a regular parametric case. On the other hand, when the true values of the SCCRAMs are either on the boundary 0 or towards 0, the empirical convergence rates of the estimators are either -1 or larger than -0.5 towards -1. This implies that the asymptotic behavior of the estimator of the SCCRAM differs substantially, depending on whether or not the true value of the SCCRAM is on the boundary 0.

According to the results for the sampling distribution and the empirical convergence rate shown in Figures S1 - S16 and Table S3, it is anticipated that the estimator of the SCCRAM is asymptotically normally distributed under a large sample size when the true value of the corresponding SCCRAM is bounded away from 0. To further explore this conjecture using the simulation results, we construct the densities of the normalized (centered and rescaled) estimates of the SCCRAMs for the cases where the true values of the SCCRAMs given in Table S1 stay away from 0 (say, larger than 0.01), the empirical rate of convergence in Table S3 is close to $n^{-0.5}$ and the total sample size is very large (say, the cell frequency is $n_c=160$ which

means $n=4320$ for $3 \times 3 \times 3$ table, $n=20000$ for $5 \times 5 \times 5$ table and $n=54880$ for $7 \times 7 \times 7$ table):

$$\begin{aligned} & n^{0.5}(\hat{\rho}_{(X_1, X_2 \rightarrow Y)}^{2*} - \rho_{0(X_1, X_2 \rightarrow Y)}^{2*}), \quad n^{0.5}(\hat{\rho}_{(X_1 \rightarrow Y)}^{2*} - \rho_{0(X_1 \rightarrow Y)}^{2*}), \quad n^{0.5}(\hat{\rho}_{(X_2 \rightarrow Y|X_1)}^{2*} - \rho_{0(X_2 \rightarrow Y|X_1)}^{2*}), \\ & n^{0.5}(\hat{\rho}_{(X_2 \rightarrow Y)}^{2*} - \rho_{0(X_2 \rightarrow Y)}^{2*}), \quad n^{0.5}(\hat{\rho}_{(X_1 \rightarrow Y|X_2)}^{2*} - \rho_{0(X_1 \rightarrow Y|X_2)}^{2*}), \end{aligned}$$

where the true values of the SCCRAMs and $n^{0.5}$ were used for centering and scaling the corresponding estimators, respectively.

The plots of the densities for the normalized estimates of the SCCRAMs above for $3 \times 3 \times 3$ table with $n=4320$ (**black colored curve**), $5 \times 5 \times 5$ table with $n=20000$ (**blue colored curve**) and $7 \times 7 \times 7$ table with $n=54880$ (**red colored curve**) are provided in

- Figure S17 - S20 for Set I-1 ~ Set I-4,
- Figure S21 - S24 for Set II-1 ~ Set II-4,
- Figure S25 - S28 for Set III-1 ~ Set III-4, and
- Figure S29 - S32 for Set IV-1 ~ Set IV-4.

From the outputs shown in Figure S17 - S32, we observe that the densities of the normalized estimates look close to a normal density with zero mean. Notice that the densities of the normalized estimates of the SCCRAMs appear to have smaller variance when the corresponding true values are closer to 0 (i.e., less than 0.1 and larger than 0.01).

S2. Simulation for SCCRAM-based permutation tests

S2.1. Design of simulation study

We design a simulation study to assess the Type I error rates/sizes and powers of the permutation tests based on the (overall/marginal/conditional) SCCRAMs in a three-way ordinal contingency table with the ordinal response variable Y and two ordinal independent variables X_1 and X_2 .

To this end, we consider three simulation factors that are the same as used in the simulation for finite sample properties of SCCRAMs shown in Section S1.1 : (i) table size (number of categories of Y , X_1 and X_2 , denoted as J , I_1 and I_2 , respectively), (ii) total sample size $n = n_c \times J \times I_1 \times I_2$ with cell frequency n_c , and (iii) magnitude of marginal and conditional associations between Y and X_1 , unconditional and conditional on X_2 , $\rho_{(X_1 \rightarrow Y)}^{2*}$ and $\rho_{(X_1 \rightarrow Y|X_2)}^{2*}$, respectively.

For each simulation factor, we use the following levels:

- three levels of table size : $3 \times 3 \times 3$, $5 \times 5 \times 5$ and $7 \times 7 \times 7$ ($J = I_1 = I_2 = 3, 5, 7$)
- six levels of the total sample size : $n = (135, 270, 540, 1080, 2160, 4320)$ for $3 \times 3 \times 3$ table, $n = (625, 1250, 2500, 5000, 10000, 20000)$ for $5 \times 5 \times 5$ table, and $n = (1715, 3430, 6860, 13720, 27440, 54880)$ for $7 \times 7 \times 7$ table from $n = n_c \times J \times I_1 \times I_2$ with $n_c = (5, 10, 20, 40, 80, 160)$
- six cases of the magnitude of marginal and conditional associations between Y and X_1 , denoted as Case 0 - Case 5 in Table S2

As to the table size and the total sample size, the same levels were used as in Section S1.1.

In order to generate an ordinal contingency table for a given combination of three simulation factors, we employed the same approach as in Section S1.1 : a latent variable approach assuming that a trivariate standard normal distribution with three pairwise correlations (r_{YX_1} , r_{YX_2} , $r_{X_1X_2}$) underlies three ordinal variables in the three-way contingency table. Note that we employed a discrete uniform distribution for the marginal distribution for each of three ordinal variables.

The three pairwise correlations in a trivariate standard normal distribution control the third factor, the magnitude of marginal and conditional associations between Y and X_1 . That is, for six cases in Table S2 representing the true values of (r_{YX_1} , r_{YX_2} , $r_{X_1X_2}$), the corresponding true values of three (overall/marginal/conditional) SCCRAMs, $\rho_{(X_1, X_2 \rightarrow Y)}^{2*}$, $\rho_{(X_1 \rightarrow Y)}^{2*}$ and $\rho_{(X_1 \rightarrow Y|X_2)}^{2*}$ are given in Table S2, denoted as $\rho_{0(X_1, X_2 \rightarrow Y)}^{2*}$, $\rho_{0(X_1 \rightarrow Y)}^{2*}$ and $\rho_{0(X_1 \rightarrow Y|X_2)}^{2*}$.

Using the sequential decomposition of $\rho_{(X_1, X_2 \rightarrow Y)}^{2*}$,

$$\rho_{(X_1, X_2 \rightarrow Y)}^{2*} = \rho_{(X_1 \rightarrow Y)}^{2*} + \rho_{(X_2 \rightarrow Y|X_1)}^{2*} = \rho_{(X_2 \rightarrow Y)}^{2*} + \rho_{(X_1 \rightarrow Y|X_2)}^{2*},$$

each of six cases in Table S2 considers scenarios designed to examine the Type I error rates/sizes and powers of the permutation tests for three individual hypotheses associated with each of three SCCRAMs, $H_0 : \rho_{(X_1, X_2 \rightarrow Y)}^{2*} = 0$, $H_0 : \rho_{(X_1 \rightarrow Y)}^{2*} = 0$ and $H_0 : \rho_{(X_1 \rightarrow Y|X_2)}^{2*} = 0$. Case 0 assumes a scenario where the true values of ($\rho_{(X_1, X_2 \rightarrow Y)}^{2*}$, $\rho_{(X_1 \rightarrow Y)}^{2*}$, $\rho_{(X_1 \rightarrow Y|X_2)}^{2*}$) are all zero and thus it focuses on the sizes of the permutation tests for three hypotheses. The scenario in Case 1 is related to a situation where $\rho_{(X_1, X_2 \rightarrow Y)}^{2*}$ is not equal to 0 while both $\rho_{(X_1 \rightarrow Y)}^{2*}$ and $\rho_{(X_1 \rightarrow Y|X_2)}^{2*}$ are both zero, so that we can study the sizes of the permutation tests for $\rho_{(X_1, X_2 \rightarrow Y)}^{2*}$ and $\rho_{(X_1 \rightarrow Y|X_2)}^{2*}$ while studying the power of the permutation test for $\rho_{(X_1 \rightarrow Y)}^{2*}$. Cases 2 - 5 are relevant to the powers of the permutation tests

for all three SSCRAMs, particularly focusing on $\rho_{(X_1 \rightarrow Y)}^{2*}$ and $\rho_{(X_1 \rightarrow Y|X_2)}^{2*}$ because the true values of $(\rho_{(X_1 \rightarrow Y)}^{2*}, \rho_{(X_1 \rightarrow Y|X_2)}^{2*})$ depart gradually from the null hypotheses of no marginal and conditional associations.

In order to estimate the sizes and powers of the permutation tests for three SSCRAMs, we first simulated 1000 three-way contingency tables for each combination of simulation factors. Then, within each simulated table, we compute the observed estimate of each of three SSCRAMs and estimate the permutation p-value using 10^6 Monte Carlo permutations under each of three null hypotheses associated with three SSCRAMs. After obtaining 1000 permutation p-values for each SSCRAM, we compute the proportion of 1000 p-values that were smaller than the pre-specified significance level α ($=0.05, 0.01$). For Case 0, the computed proportions for three SSCRAMs are the empirical sizes associated with their permutation tests. For Case 1, the computed proportions for $\rho_{(X_1 \rightarrow Y)}^{2*}$ and $\rho_{(X_1 \rightarrow Y|X_2)}^{2*}$ are the empirical sizes associated with their permutation tests while the proportions computed for $\rho_{(X_1, X_2 \rightarrow Y)}^{2*}$ is the empirical power associated with its permutation test. For Cases 2 - 5, the proportions computed for three SSCRAMs are the empirical powers associated with their permutation tests.

S2.2. Simulation results

In this section, we examine the performance of the Type I error rates/sizes and powers of the permutation tests associated with the three SSCRAMs, $\rho_{(X_1, X_2 \rightarrow Y)}^{2*}$, $\rho_{(X_1 \rightarrow Y)}^{2*}$ and $\rho_{(X_1 \rightarrow Y|X_2)}^{2*}$. Recall that a desirable test should have a good control of Type I error rate (i.e., keep Type I error rate close to the nominal level α) and produce a consistently high power under various scenarios.

To investigate the behavior of Type I error rates of the permutation tests based on three

Table S2: True values of $(r_{YX_1}, r_{YX_2}, r_{X_1X_2})$ and the corresponding true values of SCCRAMs, $\rho_{0(X_1, X_2 \rightarrow Y)}^{2*}$, $\rho_{0(X_1 \rightarrow Y)}^{2*}$, and $\rho_{0(X_1 \rightarrow Y|X_2)}^{2*}$ used in the simulation of the performance of the SCCRAMs-based permutation tests

Case	r_{YX_1}	r_{YX_2}	$r_{X_1X_2}$	Table	$\rho_{0(X_1, X_2 \rightarrow Y)}^{2*}$	$\rho_{0(X_1 \rightarrow Y)}^{2*}$	$\rho_{0(X_1 \rightarrow Y X_2)}^{2*}$
0	0	0	0	$3 \times 3 \times 3$	0	0	0
				$5 \times 5 \times 5$	0	0	0
				$7 \times 7 \times 7$	0	0	0
1	0	0.4	0	$3 \times 3 \times 3$	0.1600	0	0
				$5 \times 5 \times 5$	0.1611	0	0
				$7 \times 7 \times 7$	0.1619	0	0
2	0.158	0.4	0	$3 \times 3 \times 3$	0.1851	0.0250	0.0251
				$5 \times 5 \times 5$	0.1864	0.0252	0.0253
				$7 \times 7 \times 7$	0.1875	0.0253	0.0254
3	0.229	0.4	0	$3 \times 3 \times 3$	0.2128	0.0524	0.0528
				$5 \times 5 \times 5$	0.2143	0.0529	0.0532
				$7 \times 7 \times 7$	0.2156	0.0533	0.0536
4	0.32	0.4	0	$3 \times 3 \times 3$	0.2634	0.1023	0.1034
				$5 \times 5 \times 5$	0.2651	0.1031	0.1039
				$7 \times 7 \times 7$	0.2666	0.1038	0.1045
5	0.39	0.4	0	$3 \times 3 \times 3$	0.3140	0.1521	0.1540
				$5 \times 5 \times 5$	0.3156	0.1531	0.1545
				$7 \times 7 \times 7$	0.3175	0.1541	0.1554

SCCRAMs, we first present in Table S4 and Table S5 the empirical sizes of the permutation tests for $\rho_{(X_1 \rightarrow Y)}^{2*}$, $\rho_{(X_1 \rightarrow Y|X_2)}^{2*}$ and $\rho_{(X_1, X_2 \rightarrow Y)}^{2*}$ under the Case 0 and Case 1 scenarios, respectively. Note that Table S4 shows the empirical size of the permutation test for $\rho_{(X_1, X_2 \rightarrow Y)}^{2*}$ while Table S5 gives its empirical power. For the reference purpose, we compute the 95% binomial proportion confidence interval of α : $[0.0365, 0.0635] = 0.05 \pm 1.96 * \sqrt{0.05 * 0.95 / 1000}$ for $\alpha = 0.05$ and $[0.00383, 0.01616] = 0.01 \pm 1.96 * \sqrt{0.01 * 0.99 / 1000}$ for $\alpha = 0.01$. If the empirical size of the permutation test is within the 95% confidence interval of α , we say that the Type I error rate of the

SCCRAM-based permutation test is well-behaved. We say that it has deflated (conservative) or inflated (liberal) Type I error rate if the empirical size has a tendency to fall outside the lower or upper limits of the 95% confidence interval of α . The result given in Table S4 shows that the permutation tests for $\rho_{(X_1 \rightarrow Y)}^{2*}$, $\rho_{(X_1 \rightarrow Y|X_2)}^{2*}$ and $\rho_{(X_1, X_2 \rightarrow Y)}^{2*}$ are in general satisfactory in that both nominal levels $\alpha=0.05$ and 0.01 are well maintained in the majority of scenarios of Case 0. It would be noteworthy to mention that when the table size is small ($3 \times 3 \times 3$) and the cell frequency is not large ($n_c = 5, 10, 20$), the permutation test for marginal SSCRAM is slightly outside of the 95% confidence interval of $\alpha=0.01$. Table S5 presenting the simulation results for Case 1 shows that both nominal levels are overall well controlled for the permutation tests for $\rho_{(X_1 \rightarrow Y|X_2)}^{2*}$ and $\rho_{(X_1 \rightarrow Y)}^{2*}$ while the true value of $\rho_{(X_1, X_2 \rightarrow Y)}^{2*}$ is around 0.16 being far from 0 (its null hypothesis).

To study the power of the permutation tests concerning three SSCRAMs, we present the empirical powers of the permutation tests for $\rho_{(X_1, X_2 \rightarrow Y)}^{2*}$ in Tables S5 - S9 and $\rho_{(X_1 \rightarrow Y)}^{2*}$ and $\rho_{(X_1 \rightarrow Y|X_2)}^{2*}$ in Tables S6 - S9. As to the permutation test for $\rho_{(X_1, X_2 \rightarrow Y)}^{2*}$, we see that its empirical power is very satisfactory regardless of the table size, the total sample size n (cell frequency n_c) and the nominal levels. This is because the true values of $\rho_{(X_1, X_2 \rightarrow Y)}^{2*}$ are between about 0.16 and 0.31, which are quite far from 0 (the null hypothesis). Note that the power approaches to 1 as the magnitude of $\rho_{(X_1, X_2 \rightarrow Y)}^{2*}$ increases (i.e., from Case 1 to Case 5) even when the table size and n_c are small. Regarding the empirical powers of the permutation tests for $\rho_{(X_1 \rightarrow Y)}^{2*}$ and $\rho_{(X_1 \rightarrow Y|X_2)}^{2*}$, we make a few interesting observations from Tables S6 - S9. First, the empirical powers of the permutation tests increase and approach to 1 as the total sample size increases and/or the magnitude of marginal/conditional SSCRAMs increases from the null value of 0 for a given table size. Note

that when the total sample size (cell frequency) is small (e.g., $n_c=5$ and/or 10), the magnitude of marginal/conditional SCCRAMs is about 0.025 and/or 0.05 and the size of the table is $3 \times 3 \times 3$, the permutation tests for both $\rho_{(X_1 \rightarrow Y)}^{2*}$ and $\rho_{(X_1 \rightarrow Y|X_2)}^{2*}$ appear to have low power. Second, the powers of the permutation tests also increase to 1 as the table size increases at any given combination of the other two simulation factors, and this holds even when the cell frequency and the magnitude of marginal/conditional SCCRAMs are small. Third, given that the true values of $\rho_{(X_1 \rightarrow Y)}^{2*}$ and $\rho_{(X_1 \rightarrow Y|X_2)}^{2*}$ are very similar each other in each case of Table S2, the power of the permutation test for $\rho_{(X_1 \rightarrow Y)}^{2*}$ tends to be equal to or higher than that of $\rho_{(X_1 \rightarrow Y|X_2)}^{2*}$ under each combination of the simulation factors.

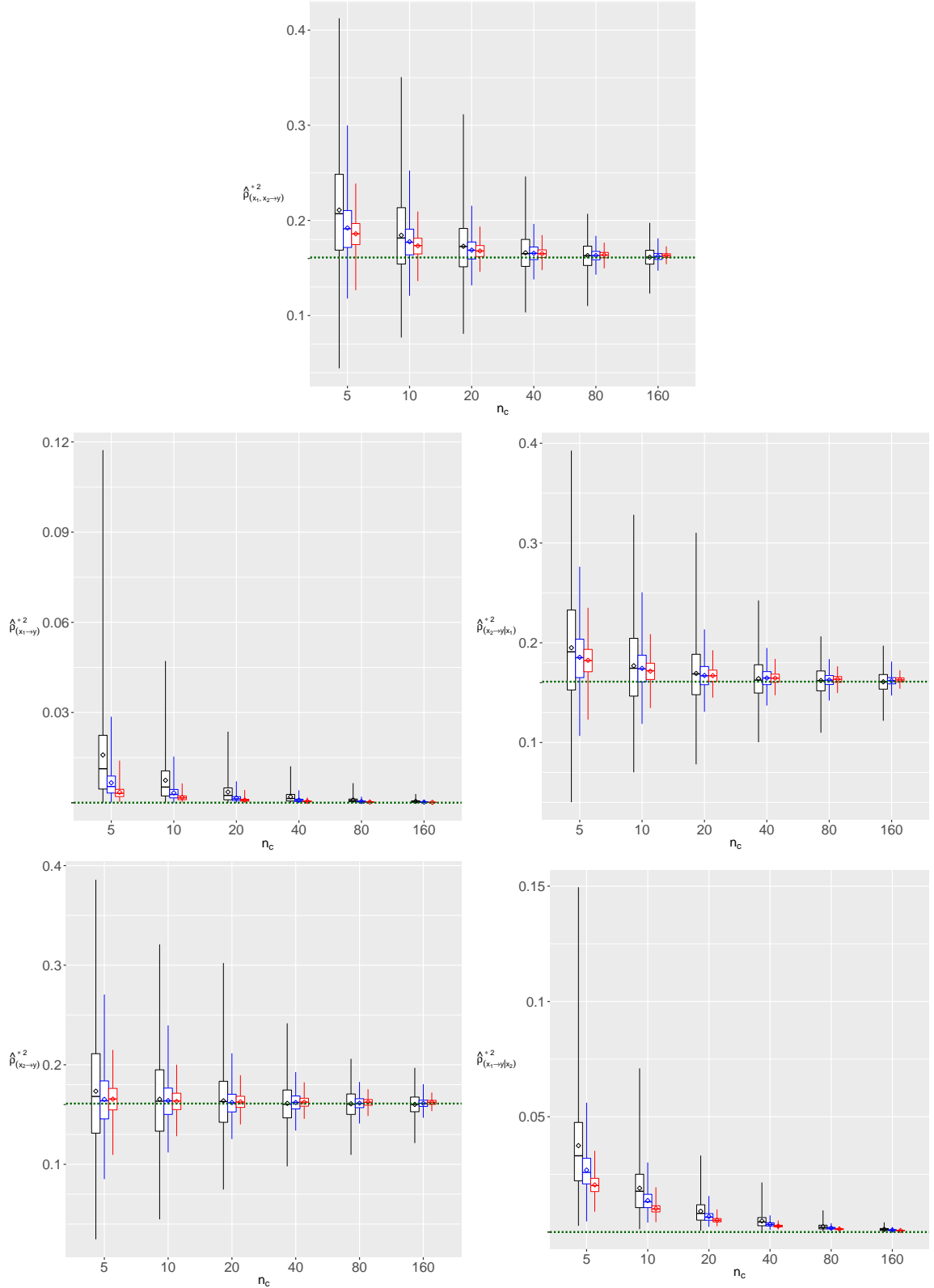


Fig. S1: Set I-1 : Boxplots of $\hat{\rho}^{*2}_{(X_1, X_2 \rightarrow Y)}$ (first row), $\hat{\rho}^{*2}_{(X_1 \rightarrow Y)}$ (left in the second row), $\hat{\rho}^{*2}_{(X_2 \rightarrow Y | X_1)}$ (right in the second row), $\hat{\rho}^{*2}_{(X_2 \rightarrow Y)}$ (left in the third row), and $\hat{\rho}^{*2}_{(X_1 \rightarrow Y | X_2)}$ (right in the third row) for the cell counts $n_c = (5, 10, 20, 40, 80, 160)$ under $3 \times 3 \times 3$ table (black colored boxplot), $5 \times 5 \times 5$ table (blue colored boxplot) and $7 \times 7 \times 7$ table (red colored boxplot)

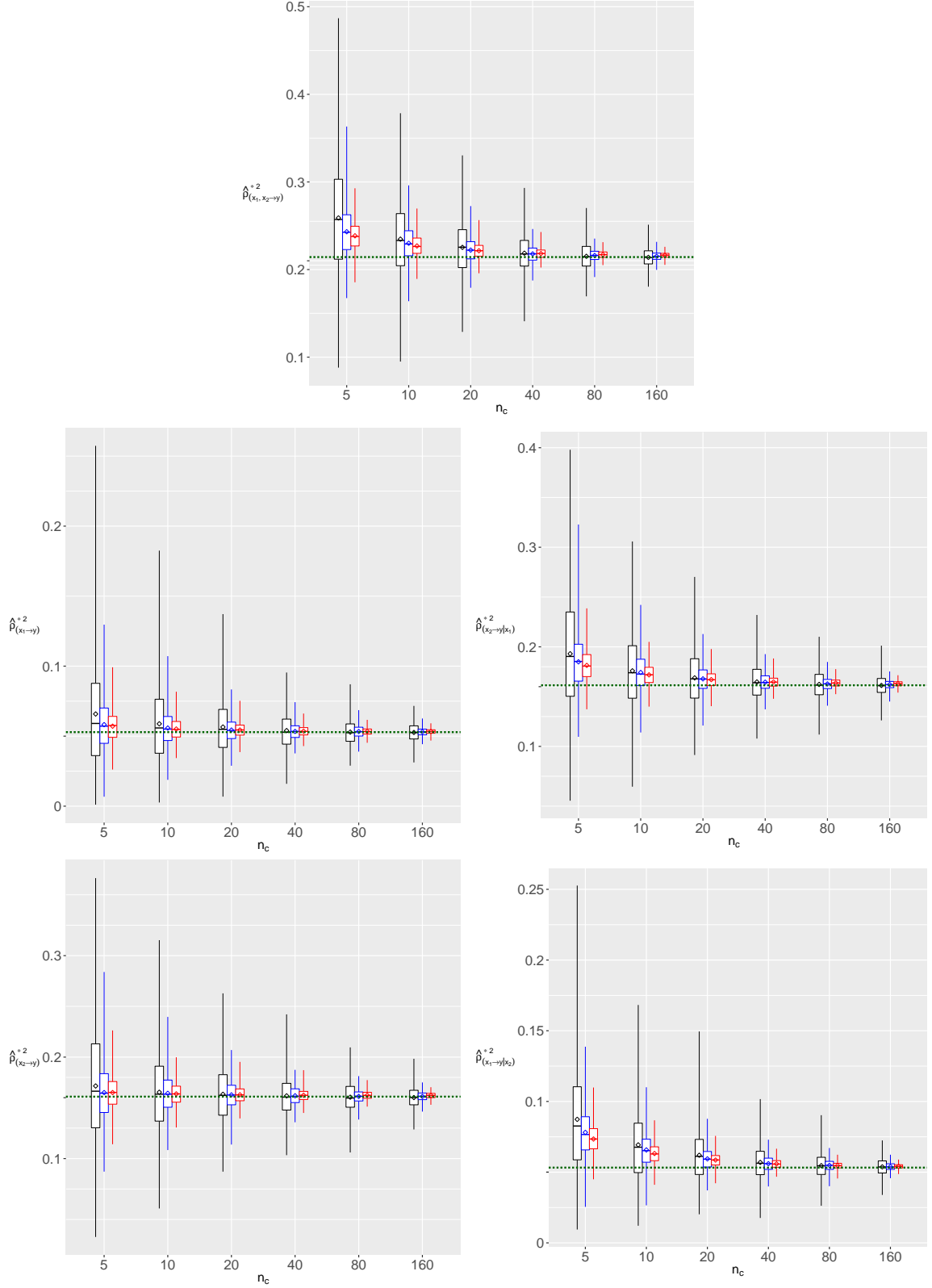


Fig. S2: Set I-2 : Boxplots of $\hat{\rho}_{(x_1, x_2 \rightarrow y)}^{*2}$ (first row), $\hat{\rho}_{(x_1 \rightarrow y)}^{*2}$ (left in the second row), $\hat{\rho}_{(x_2 \rightarrow y|x_1)}^{*2}$ (right in the second row), $\hat{\rho}_{(x_2 \rightarrow y)}^{*2}$ (left in the third row), and $\hat{\rho}_{(x_1 \rightarrow y|x_2)}^{*2}$ (right in the third row) for the cell counts $n_c = (5, 10, 20, 40, 80, 160)$ under $3 \times 3 \times 3$ table (black colored boxplot), $5 \times 5 \times 5$ table (blue colored boxplot) and $7 \times 7 \times 7$ table (red colored boxplot)

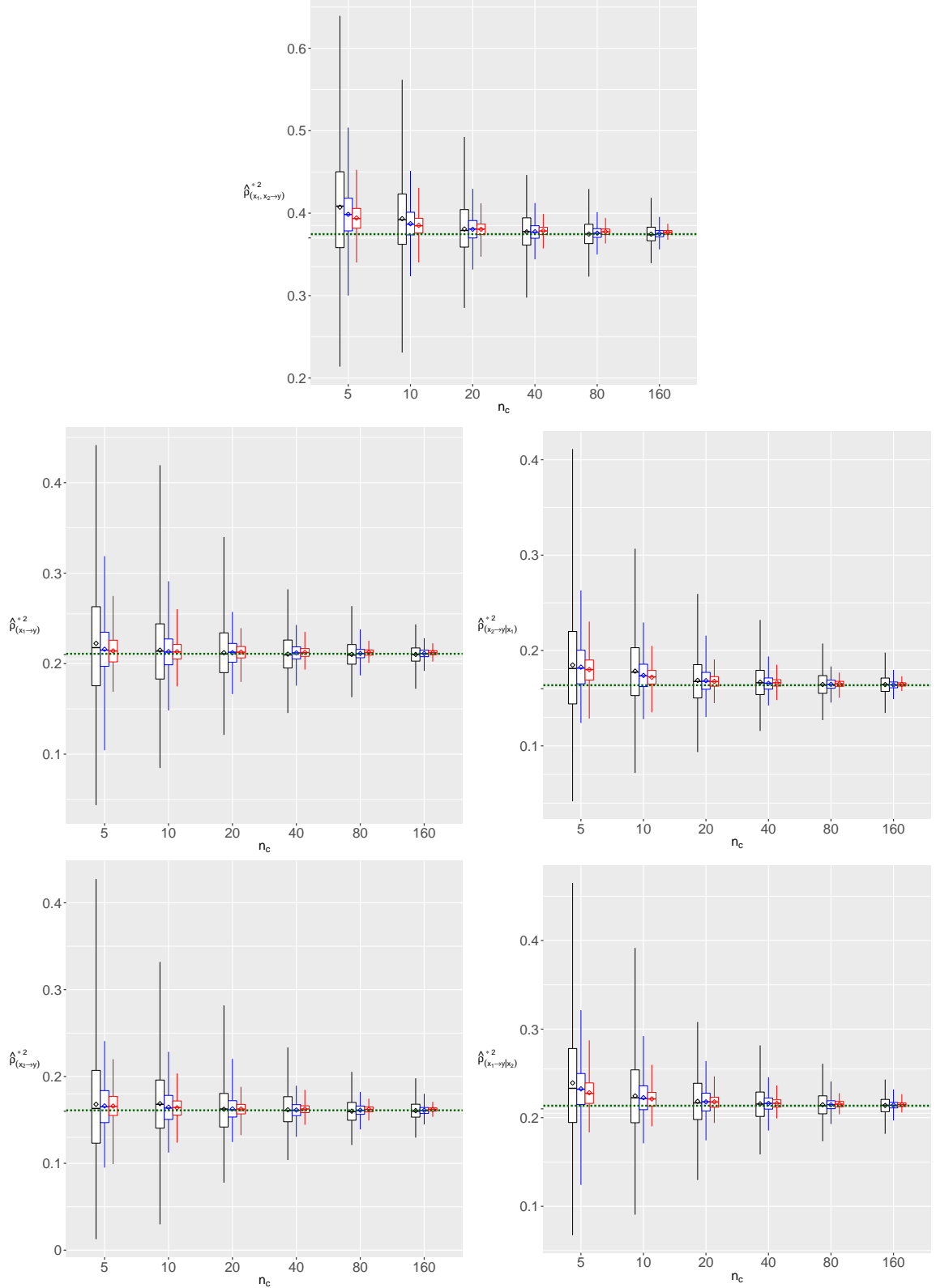


Fig. S3: Set I-3 : Boxplots of $\hat{\rho}_{(x_1, x_2 \rightarrow y)}^{*2}$ (first row), $\hat{\rho}_{(x_1 \rightarrow y)}^{*2}$ (left in the second row), $\hat{\rho}_{(x_2 \rightarrow y|x_1)}^{*2}$ (right in the second row), $\hat{\rho}_{(x_1 \rightarrow y|x_2)}^{*2}$ (left in the third row), and $\hat{\rho}_{(x_1 \rightarrow y|x_2)}^{*2}$ (right in the third row) for the cell counts $n_c = (5, 10, 20, 40, 80, 160)$ under $3 \times 3 \times 3$ table (black colored boxplot), $5 \times 5 \times 5$ table (blue colored boxplot) and $7 \times 7 \times 7$ table (red colored boxplot) .

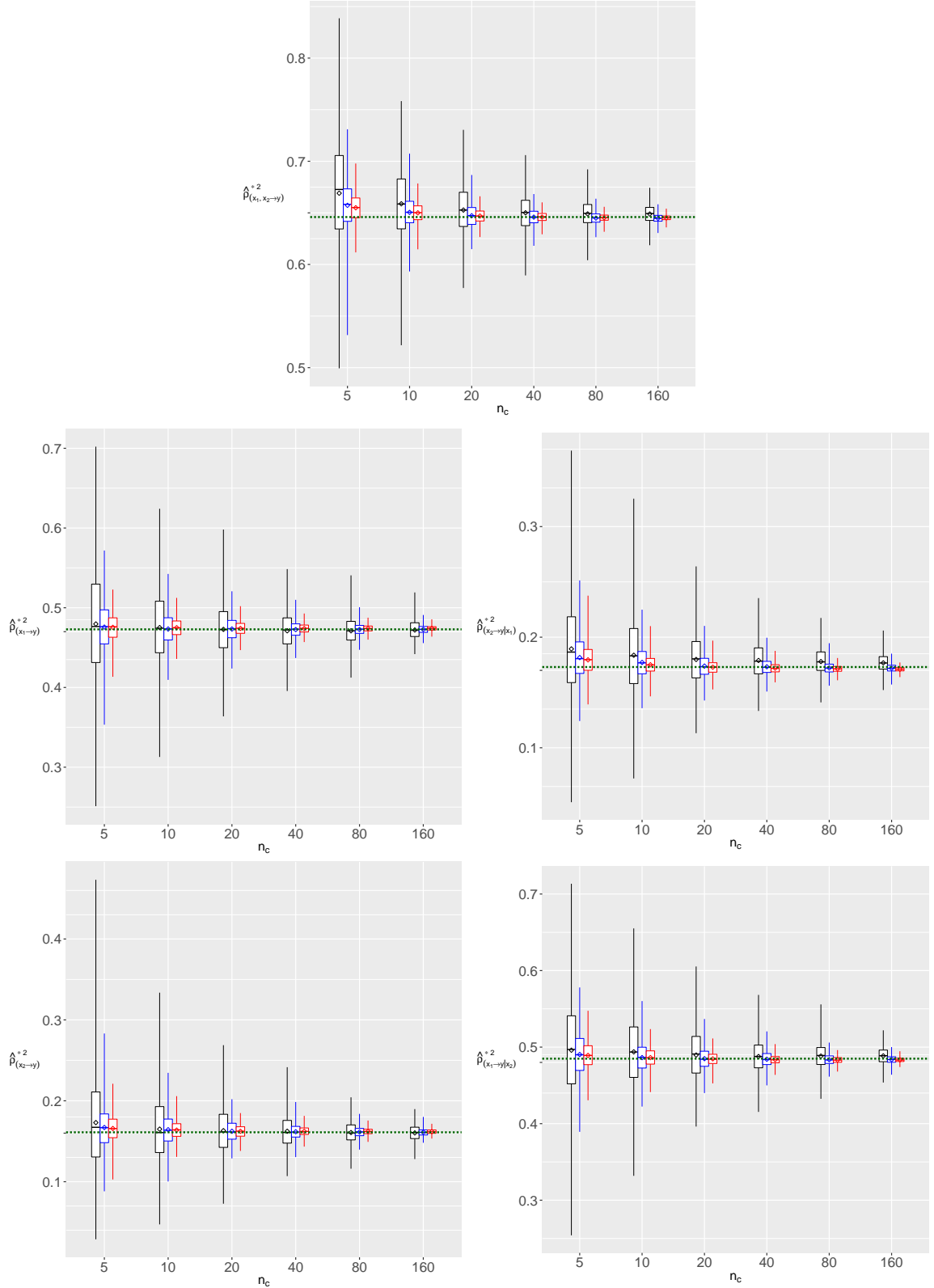


Fig. S4: Set I-4 : Boxplots of $\hat{\rho}_{(x_1, x_2 \rightarrow y)}^{*2}$ (first row), $\hat{\rho}_{(x_1 \rightarrow y)}^{*2}$ (left in the second row), $\hat{\rho}_{(x_2 \rightarrow y|x_1)}^{*2}$ (right in the second row), $\hat{\rho}_{(x_1 \rightarrow y|x_2)}^{*2}$ (left in the third row), and $\hat{\rho}_{(x_1 \rightarrow y|x_2)}^{*2}$ (right in the third row) for the cell counts $n_c = (5, 10, 20, 40, 80, 160)$ under $3 \times 3 \times 3$ table (black colored boxplot), $5 \times 5 \times 5$ table (blue colored boxplot) and $7 \times 7 \times 7$ table (red colored boxplot)

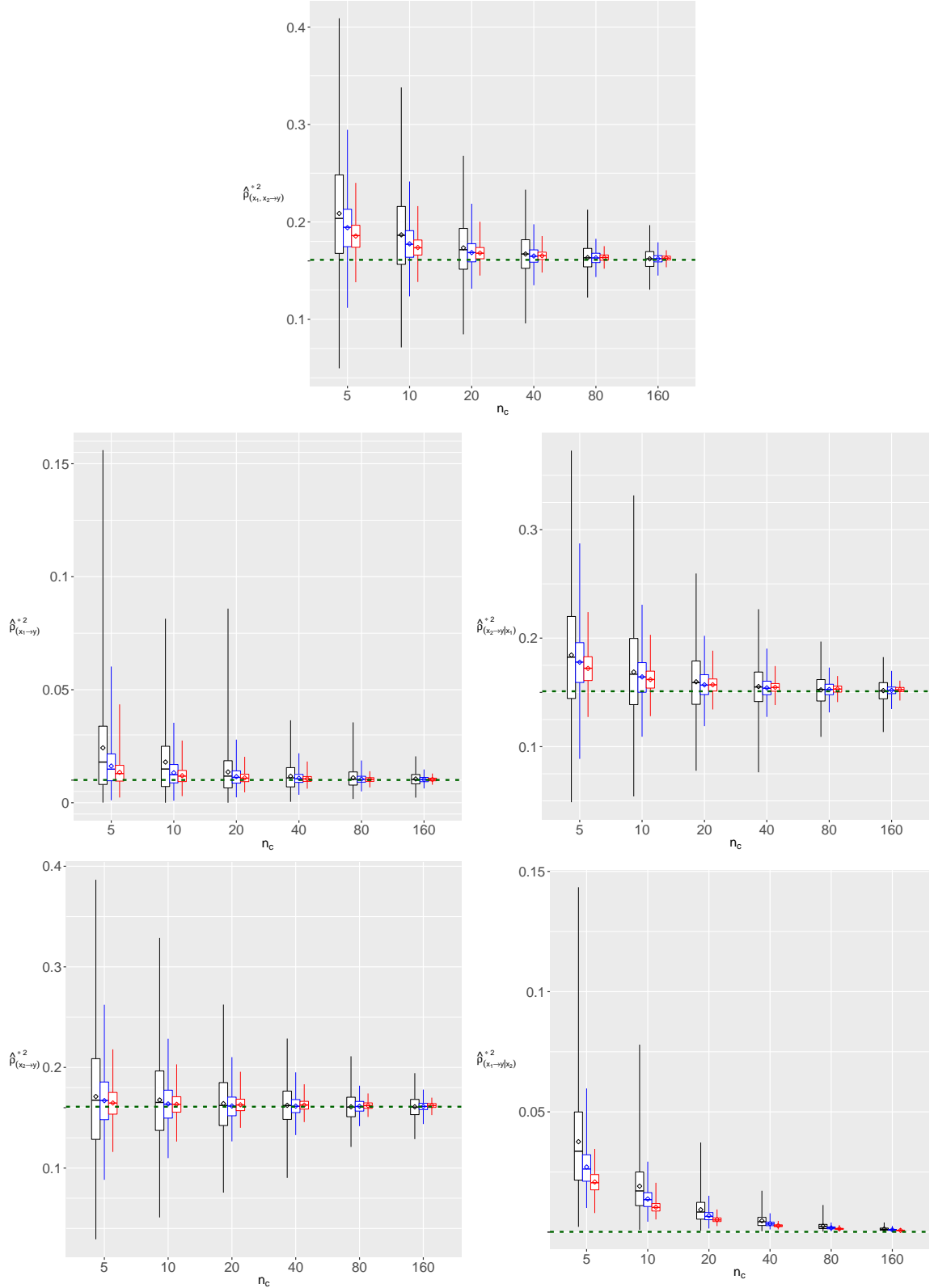


Fig. S5: Set II-1 : Boxplots of $\hat{\rho}^{*2}_{(x_1, x_2 \rightarrow y)}$ (first row), $\hat{\rho}^{*2}_{(x_1 \rightarrow y)}$ (left in the second row), $\hat{\rho}^{*2}_{(x_2 \rightarrow y|x_1)}$ (right in the second row), $\hat{\rho}^{*2}_{(x_2 \rightarrow y)}$ (left in the third row), and $\hat{\rho}^{*2}_{(x_1 \rightarrow y|x_2)}$ (right in the third row) for the cell counts $n_c = (5, 10, 20, 40, 80, 160)$ under $3 \times 3 \times 3$ table (black colored boxplot), $5 \times 5 \times 5$ table (blue colored boxplot) and $7 \times 7 \times 7$ table (red colored boxplot)

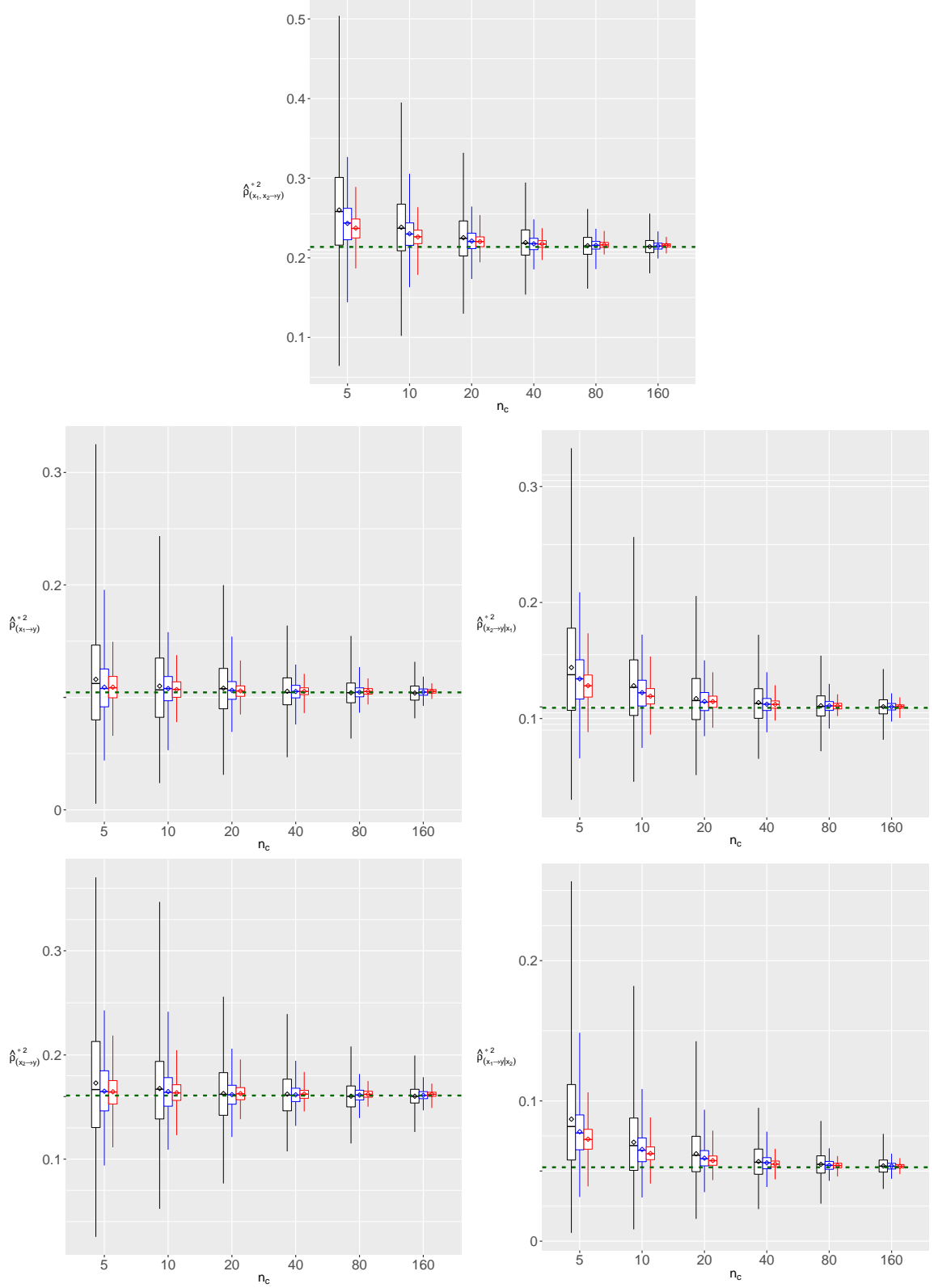


Fig. S6: Set II-2 : Boxplots of $\hat{\rho}_{(x_1, x_2 \rightarrow y)}^{*2}$ (first row), $\hat{\rho}_{(x_1 \rightarrow y)}^{*2}$ (left in the second row), $\hat{\rho}_{(x_2 \rightarrow y|x_1)}^{*2}$ (right in the second row), $\hat{\rho}_{(x_2 \rightarrow y)}^{*2}$ (left in the third row), and $\hat{\rho}_{(x_1 \rightarrow y|x_2)}^{*2}$ (right in the third row) for the cell counts $n_c = (5, 10, 20, 40, 80, 160)$ under $3 \times 3 \times 3$ table (black colored boxplot), $5 \times 5 \times 5$ table (blue colored boxplot) and $7 \times 7 \times 7$ table (red colored boxplot)

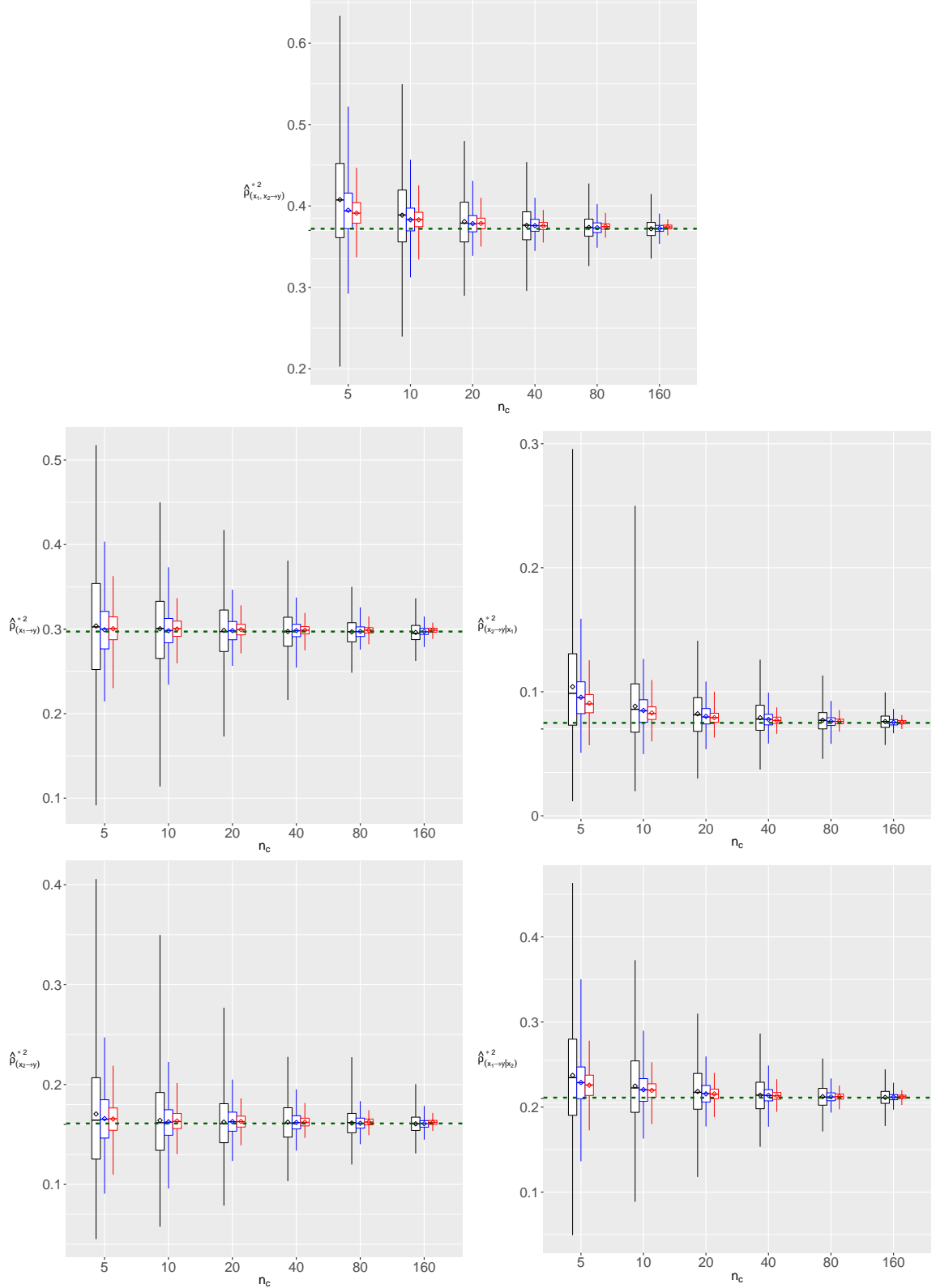


Fig. S7: Set II-3 : Boxplots of $\hat{\rho}_{(x_1, x_2 \rightarrow y)}^{*2}$ (first row), $\hat{\rho}_{(x_1 \rightarrow y)}^{*2}$ (left in the second row), $\hat{\rho}_{(x_2 \rightarrow y|x_1)}^{*2}$ (right in the second row), $\hat{\rho}_{(x_2 \rightarrow y)}^{*2}$ (left in the third row), and $\hat{\rho}_{(x_1 \rightarrow y|x_2)}^{*2}$ (right in the third row) for the cell counts $n_c = (5, 10, 20, 40, 80, 160)$ under $3 \times 3 \times 3$ table (black colored boxplot), $5 \times 5 \times 5$ table (blue colored boxplot) and $7 \times 7 \times 7$ table (red colored boxplot)

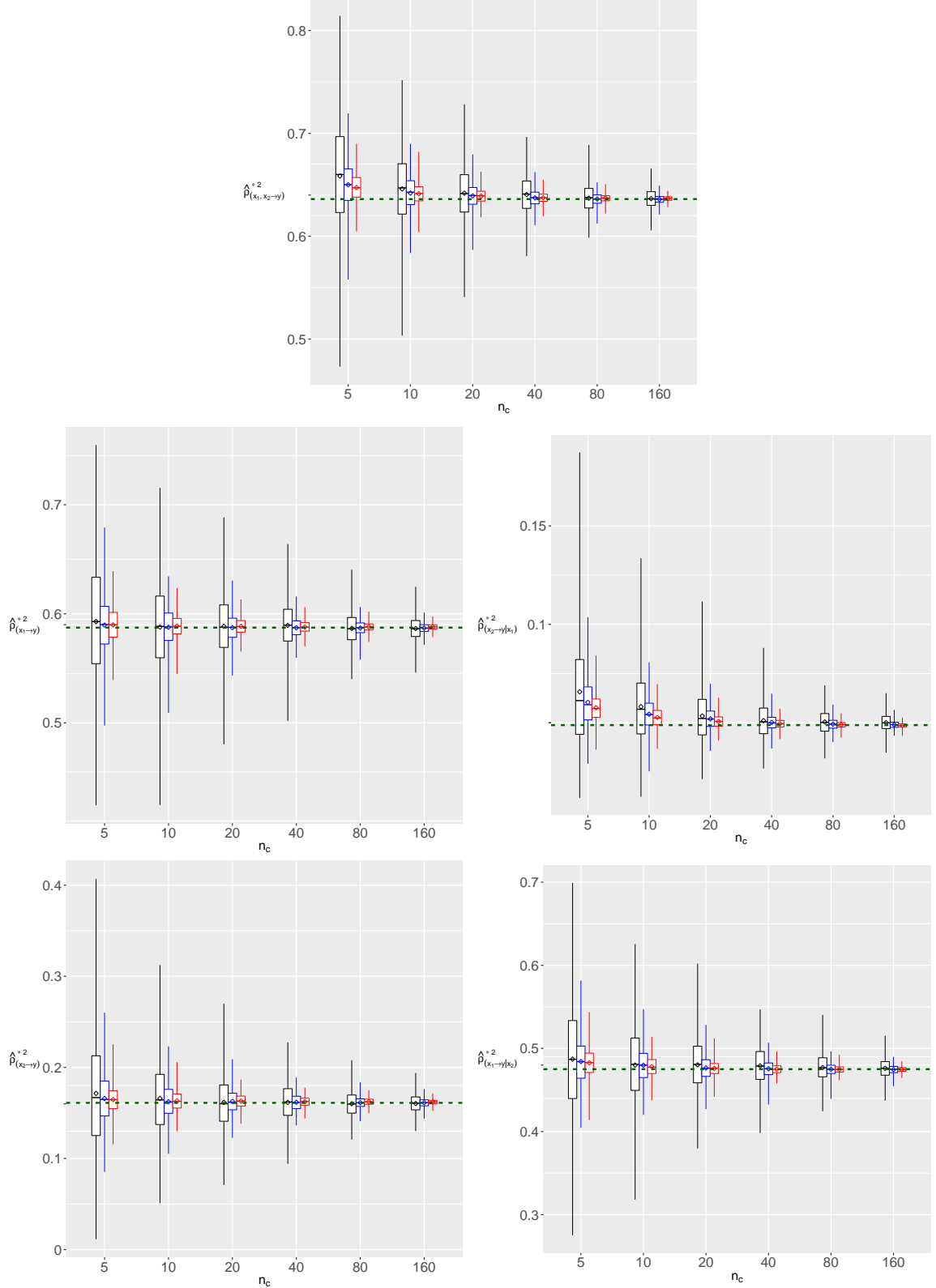


Fig. S8: Set II-4 : Boxplots of $\hat{\rho}_{(x_1, x_2 \rightarrow y)}^{*2}$ (first row), $\hat{\rho}_{(x_1 \rightarrow y)}^{*2}$ (left in the second row), $\hat{\rho}_{(x_2 \rightarrow y|x_1)}^{*2}$ (right in the second row), $\hat{\rho}_{(x_2 \rightarrow y)}^{*2}$ (left in the third row), and $\hat{\rho}_{(x_1 \rightarrow y|x_2)}^{*2}$ (right in the third row) for the cell counts $n_c = (5, 10, 20, 40, 80, 160)$ under $3 \times 3 \times 3$ table (black colored boxplot), $5 \times 5 \times 5$ table (blue colored boxplot) and $7 \times 7 \times 7$ table (red colored boxplot)

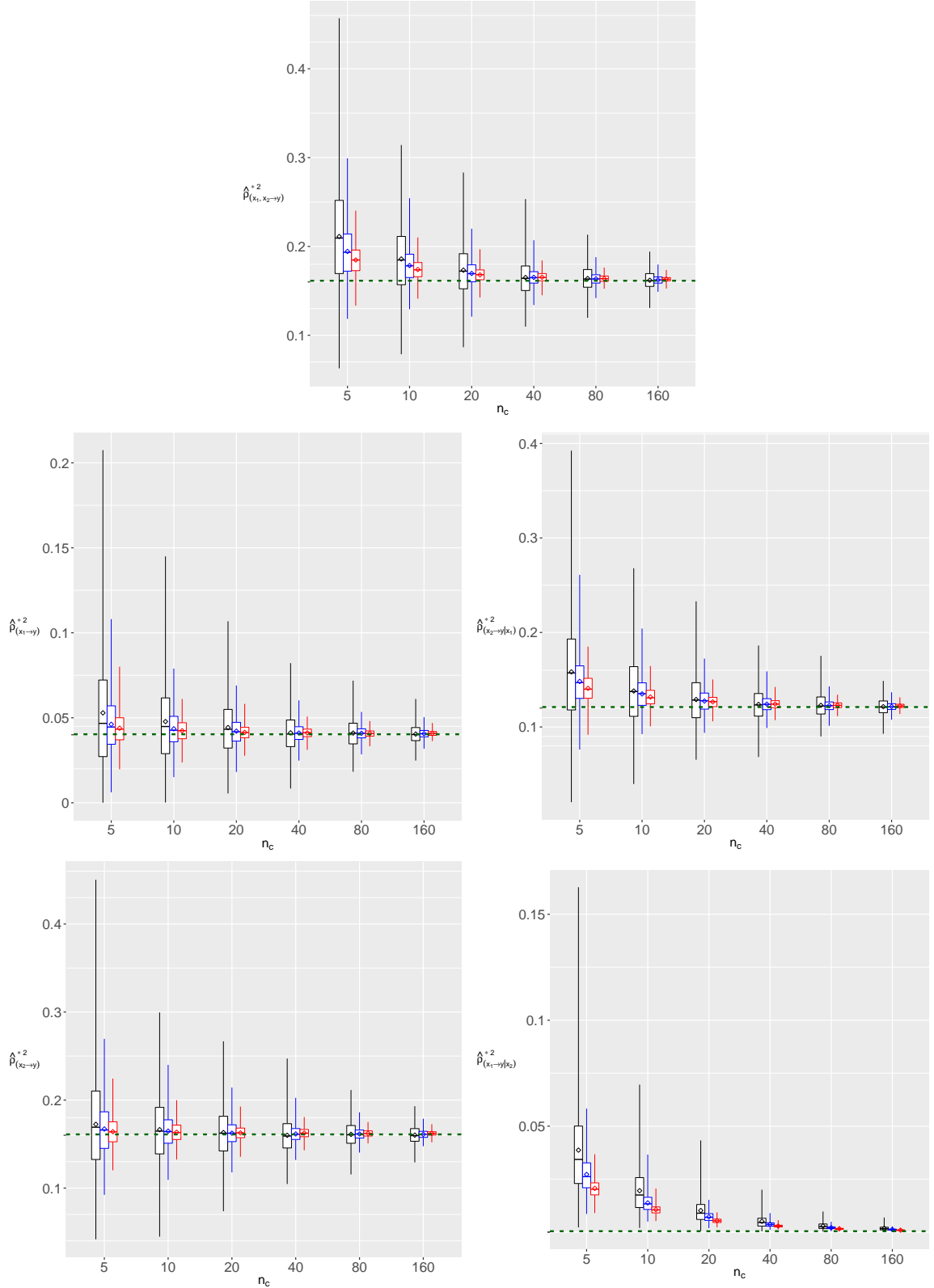


Fig. S9: Set III-1 : Boxplots of $\hat{\rho}_{(X_1, X_2 \rightarrow Y)}^{*2}$ (first row), $\hat{\rho}_{(X_1 \rightarrow Y)}^{*2}$ (left in the second row), $\hat{\rho}_{(X_2 \rightarrow Y|X_1)}^{*2}$ (right in the second row), $\hat{\rho}_{(X_2 \rightarrow Y)}^{*2}$ (left in the third row), and $\hat{\rho}_{(X_1 \rightarrow Y|X_2)}^{*2}$ (right in the third row) for the cell counts $n_c = (5, 10, 20, 40, 80, 160)$ under $3 \times 3 \times 3$ table (black colored boxplot), $5 \times 5 \times 5$ table (blue colored boxplot) and $7 \times 7 \times 7$ table (red colored boxplot)

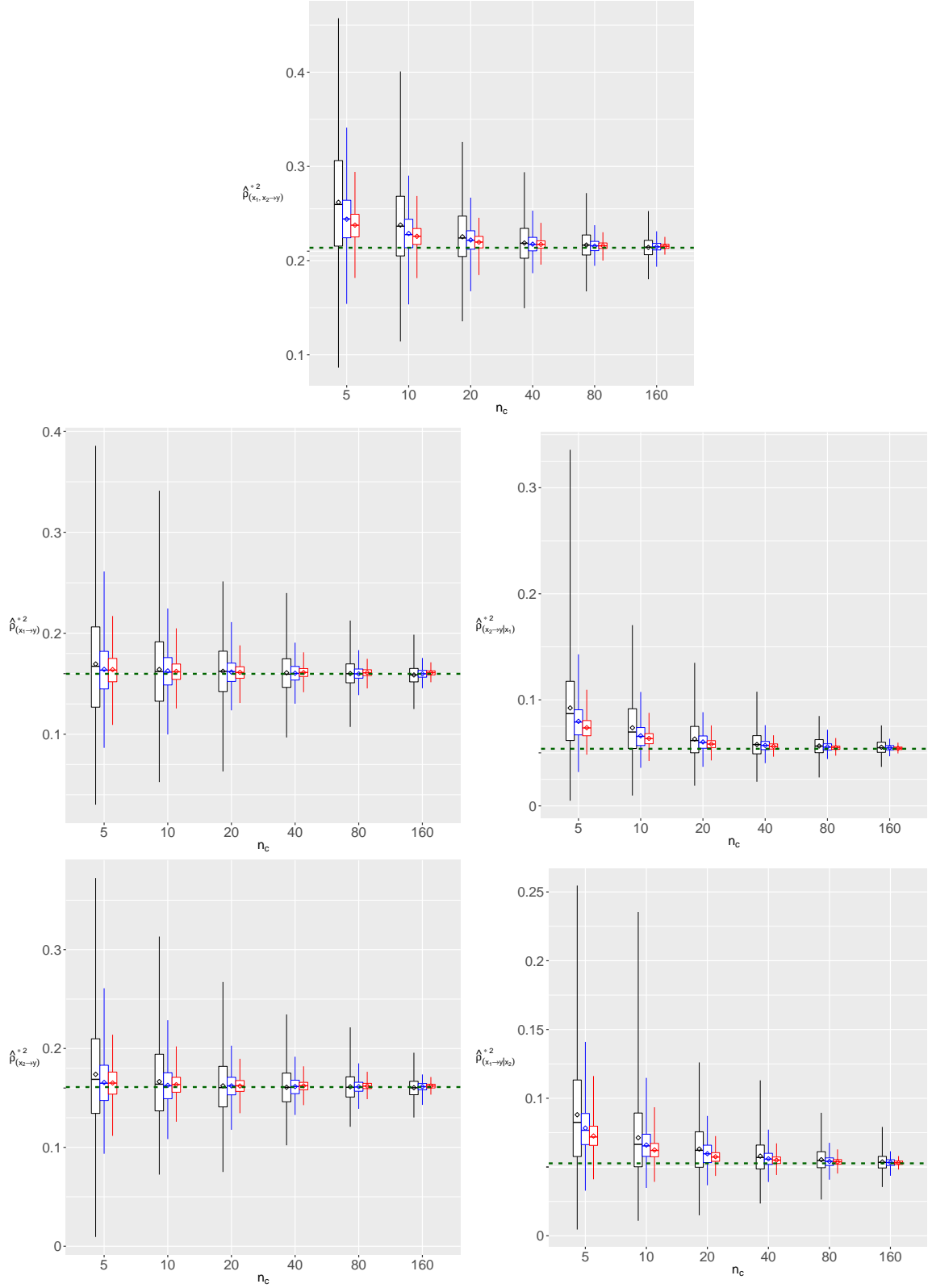


Fig. S10: Set III-2 : Boxplots of $\hat{\rho}_{(X_1, X_2 \rightarrow Y)}^{2*}$ (first row), $\hat{\rho}_{(X_1 \rightarrow Y)}^{2*}$ (left in the second row), $\hat{\rho}_{(X_2 \rightarrow Y|X_1)}^{2*}$ (right in the second row), $\hat{\rho}_{(X_2 \rightarrow Y)}^{2*}$ (left in the third row), and $\hat{\rho}_{(X_1 \rightarrow Y|X_2)}^{2*}$ (right in the third row) for the cell counts $n_c = (5, 10, 20, 40, 80, 160)$ under $3 \times 3 \times 3$ table (black colored boxplot), $5 \times 5 \times 5$ table (blue colored boxplot) and $7 \times 7 \times 7$ table (red colored boxplot)

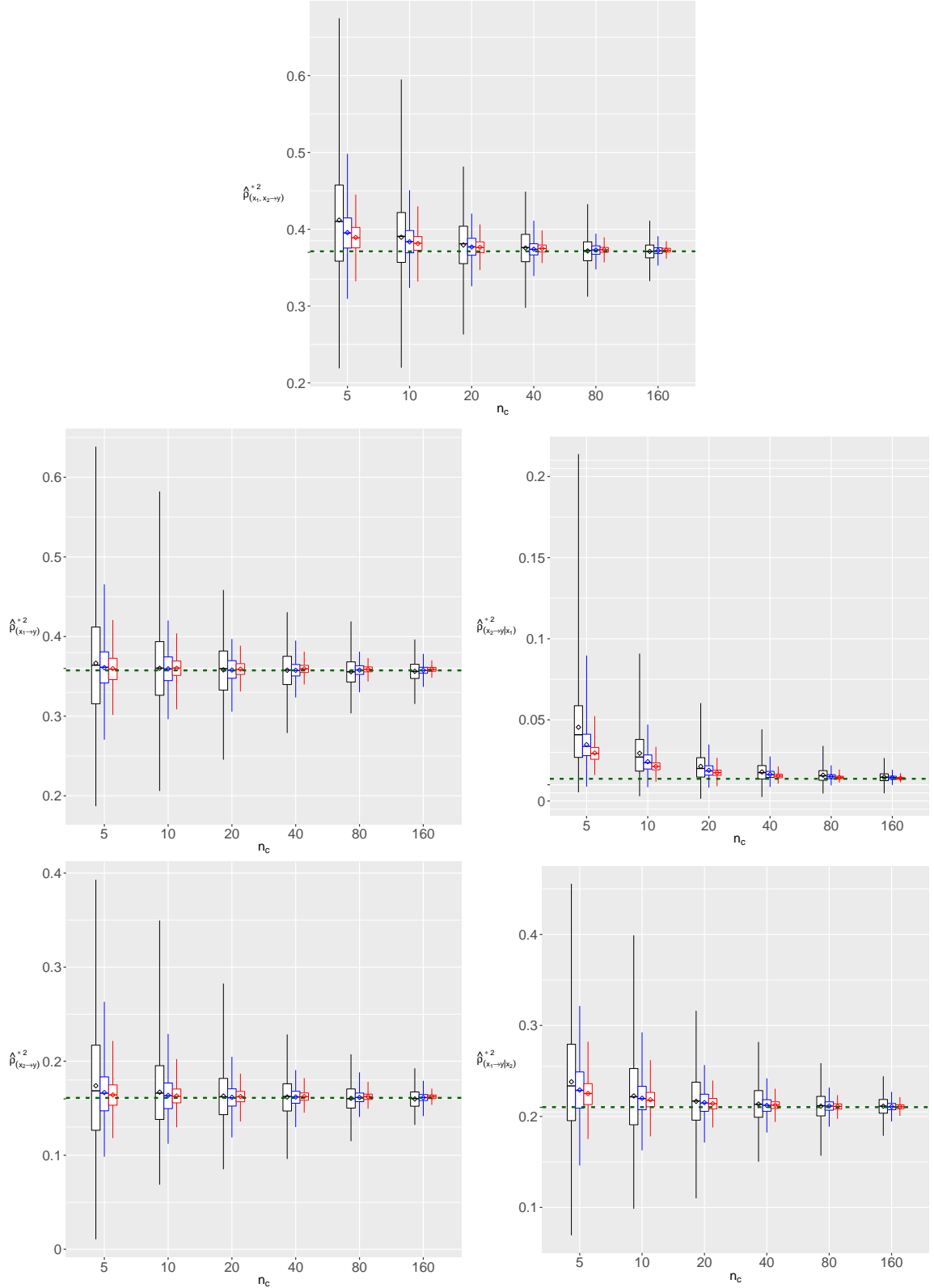


Fig. S11: Set III-3 : Boxplots of $\hat{\rho}_{(x_1, x_2 \rightarrow y)}^{*2}$ (first row), $\hat{\rho}_{(x_1 \rightarrow y)}^{*2}$ (left in the second row), $\hat{\rho}_{(x_2 \rightarrow y|x_1)}^{*2}$ (right in the second row), $\hat{\rho}_{(x_2 \rightarrow y)}^{*2}$ (left in the third row), and $\hat{\rho}_{(x_1 \rightarrow y|x_2)}^{*2}$ (right in the third row) for the cell counts $n_c = (5, 10, 20, 40, 80, 160)$ under $3 \times 3 \times 3$ table (black colored boxplot), $5 \times 5 \times 5$ table (blue colored boxplot) and $7 \times 7 \times 7$ table (red colored boxplot)

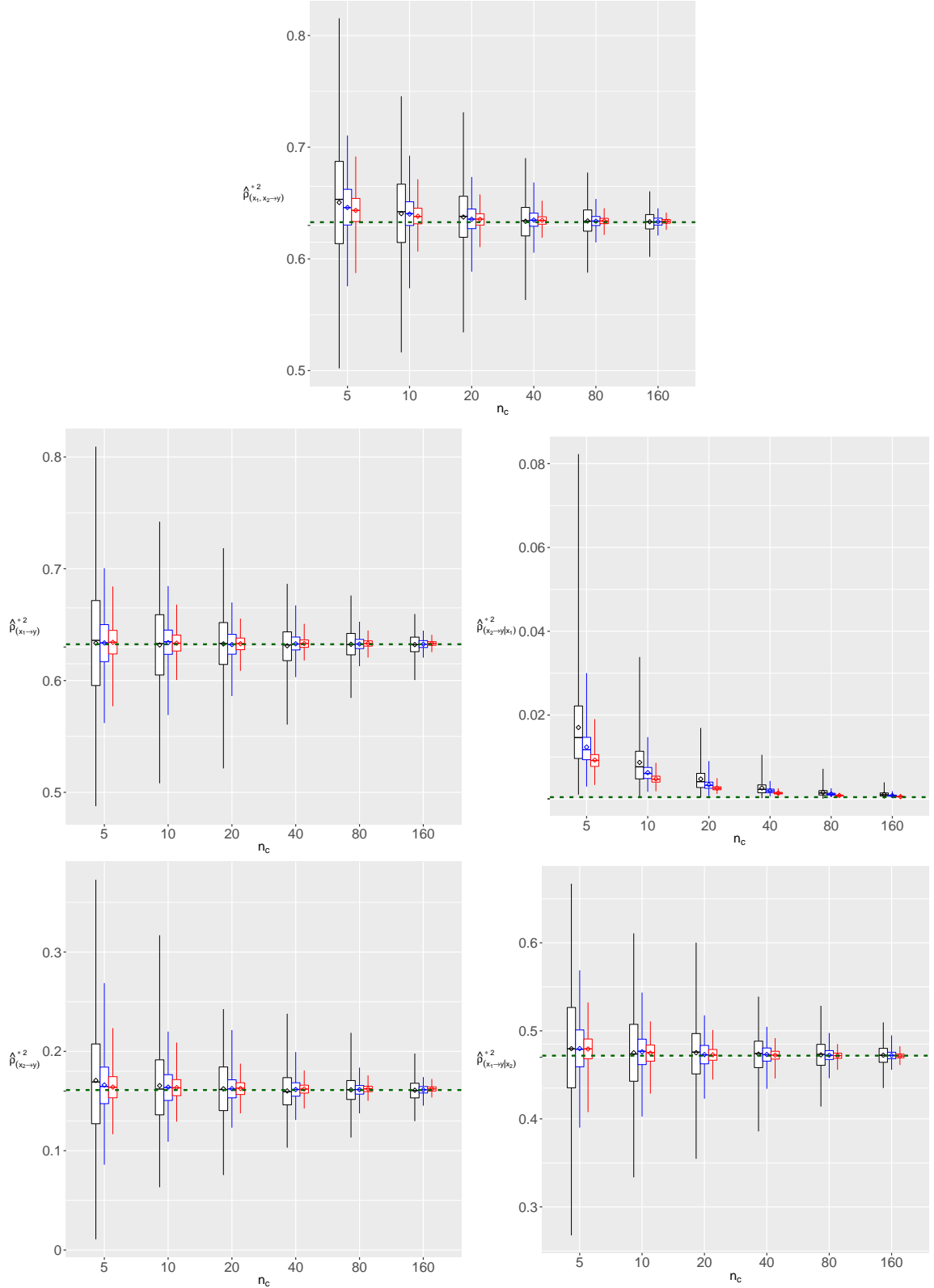


Fig. S12: Set III-4 : Boxplots of $\hat{\rho}_{(X_1, X_2 \rightarrow Y)}^{*2}$ (first row), $\hat{\rho}_{(X_1 \rightarrow Y)}^{*2}$ (left in the second row), $\hat{\rho}_{(X_2 \rightarrow Y|X_1)}^{*2}$ (right in the second row), $\hat{\rho}_{(X_2 \rightarrow Y)}^{*2}$ (left in the third row), and $\hat{\rho}_{(X_1 \rightarrow Y|X_2)}^{*2}$ (right in the third row) for the cell counts $n_c = (5, 10, 20, 40, 80, 160)$ under $3 \times 3 \times 3$ table (black colored boxplot), $5 \times 5 \times 5$ table (blue colored boxplot) and $7 \times 7 \times 7$ table (red colored boxplot)

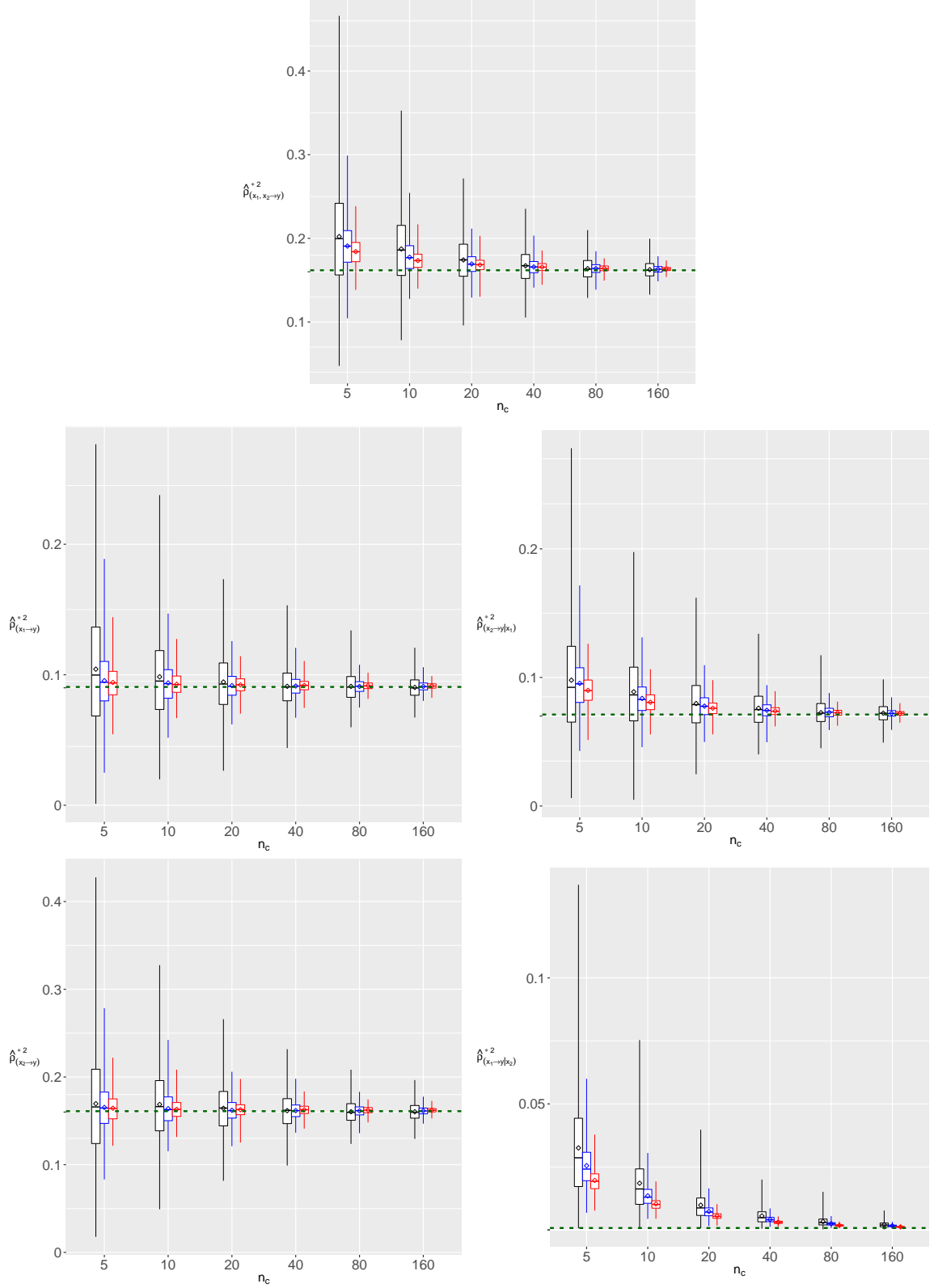


Fig. S13: Set IV-1 : Boxplots of $\hat{\rho}_{(x_1, x_2 \rightarrow y)}^{*2}$ (first row), $\hat{\rho}_{(x_1 \rightarrow y)}^{*2}$ (left in the second row), $\hat{\rho}_{(x_2 \rightarrow y|x_1)}^{*2}$ (right in the second row), $\hat{\rho}_{(x_2 \rightarrow y)}^{*2}$ (left in the third row), and $\hat{\rho}_{(x_1 \rightarrow y|x_2)}^{*2}$ (right in the third row) for the cell counts $n_c = (5, 10, 20, 40, 80, 160)$ under $3 \times 3 \times 3$ table (black colored boxplot), $5 \times 5 \times 5$ table (blue colored boxplot) and $7 \times 7 \times 7$ table (red colored boxplot)

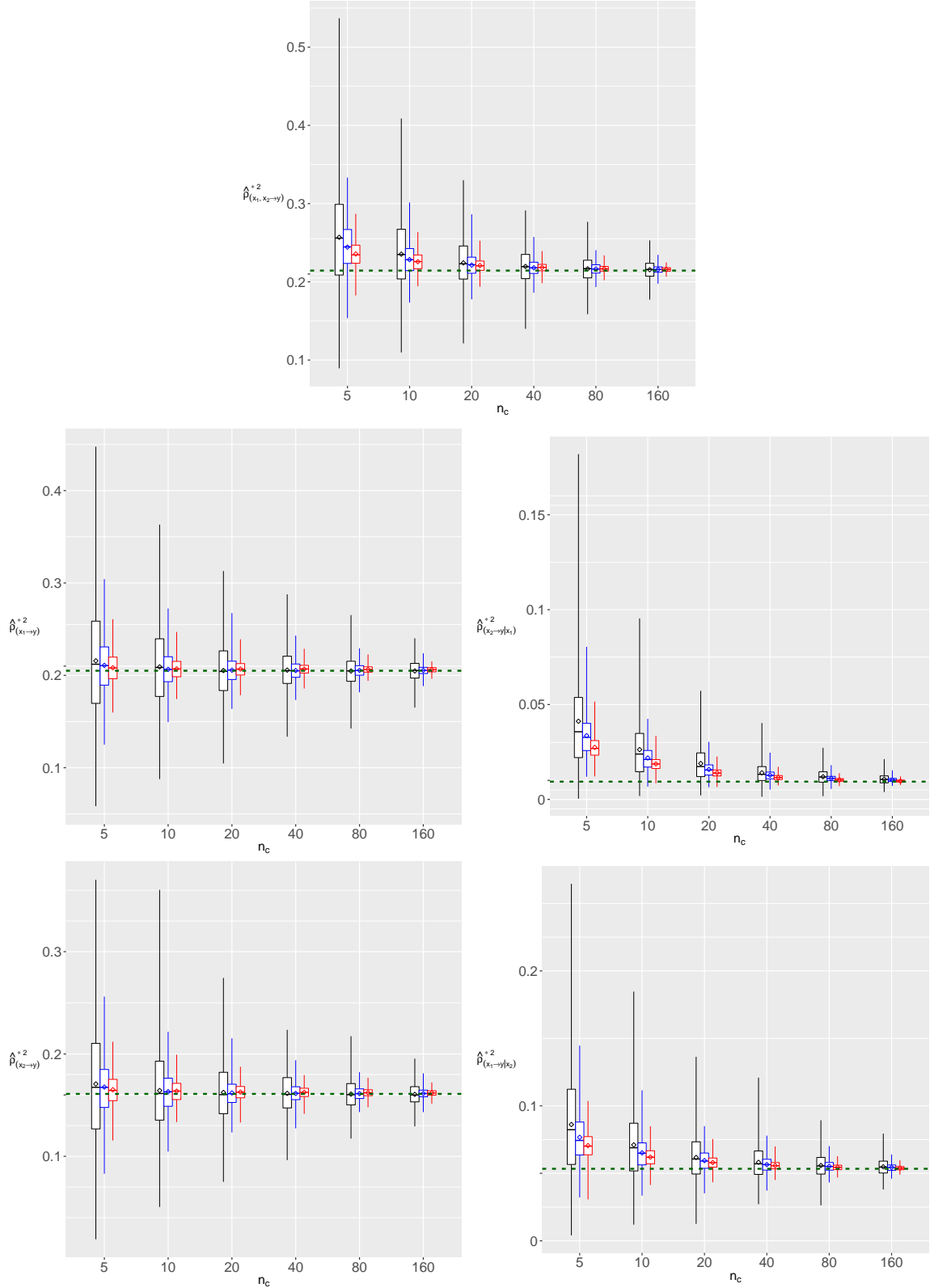


Fig. S14: Set IV-2 : Boxplots of $\hat{\rho}_{(x_1, x_2 \rightarrow y)}^{*2}$ (first row), $\hat{\rho}_{(x_1 \rightarrow y)}^{*2}$ (left in the second row), $\hat{\rho}_{(x_2 \rightarrow y|x_1)}^{*2}$ (right in the second row), $\hat{\rho}_{(x_2 \rightarrow y)}^{*2}$ (left in the third row), and $\hat{\rho}_{(x_1 \rightarrow y|x_2)}^{*2}$ (right in the third row) for the cell counts $n_c = (5, 10, 20, 40, 80, 160)$ under $3 \times 3 \times 3$ table (black colored boxplot), $5 \times 5 \times 5$ table (blue colored boxplot) and $7 \times 7 \times 7$ table (red colored boxplot)

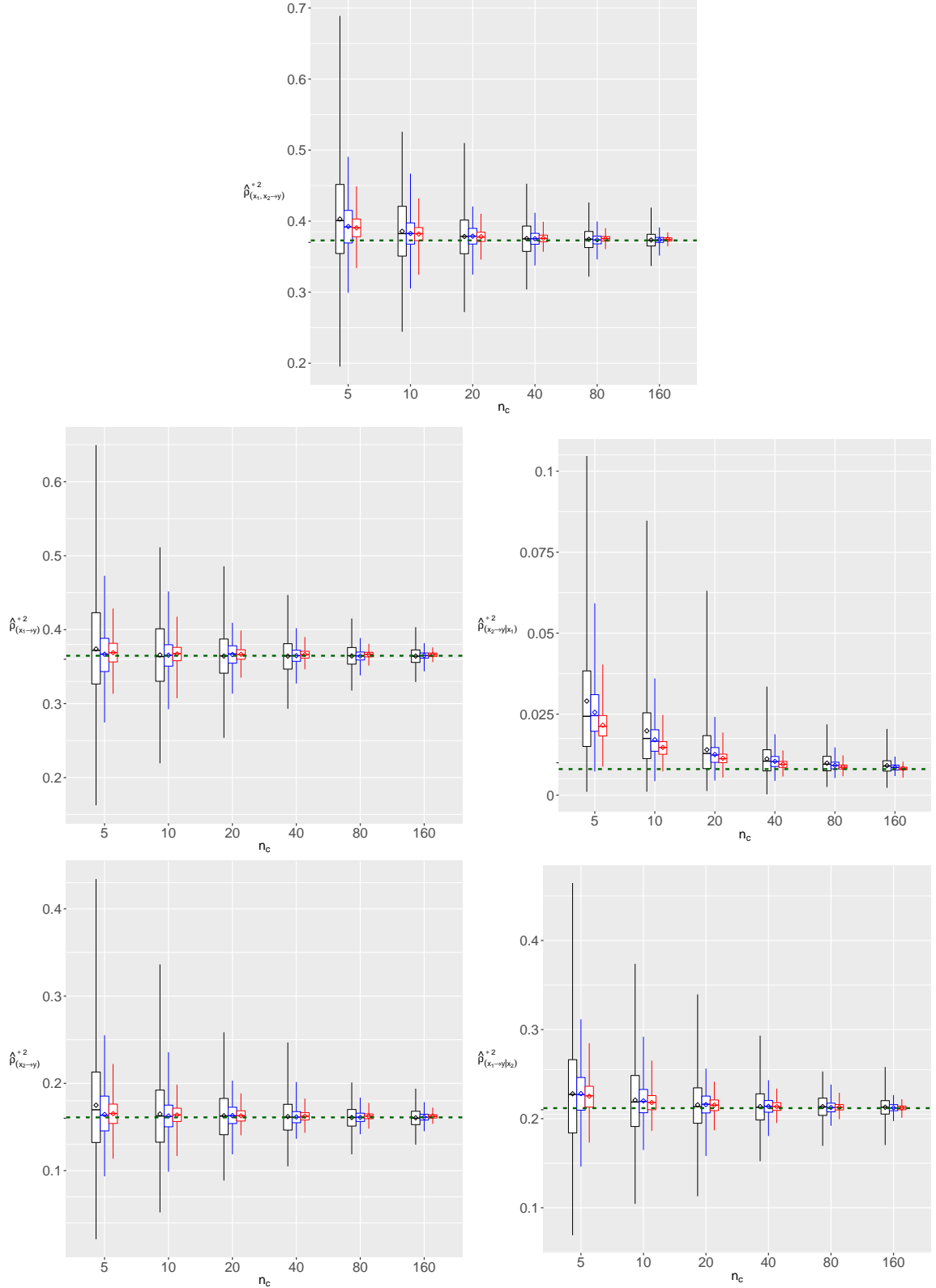


Fig. S15: Set IV-3 : Boxplots of $\hat{\rho}_{(x_1, x_2 \rightarrow y)}^{*2}$ (first row), $\hat{\rho}_{(x_1 \rightarrow y)}^{*2}$ (left in the second row), $\hat{\rho}_{(x_2 \rightarrow y|x_1)}^{*2}$ (right in the second row), $\hat{\rho}_{(x_2 \rightarrow y)}^{*2}$ (left in the third row), and $\hat{\rho}_{(x_1 \rightarrow y|x_2)}^{*2}$ (right in the third row) for the cell counts $n_c = (5, 10, 20, 40, 80, 160)$ under $3 \times 3 \times 3$ table (black colored boxplot), $5 \times 5 \times 5$ table (blue colored boxplot) and $7 \times 7 \times 7$ table (red colored boxplot)

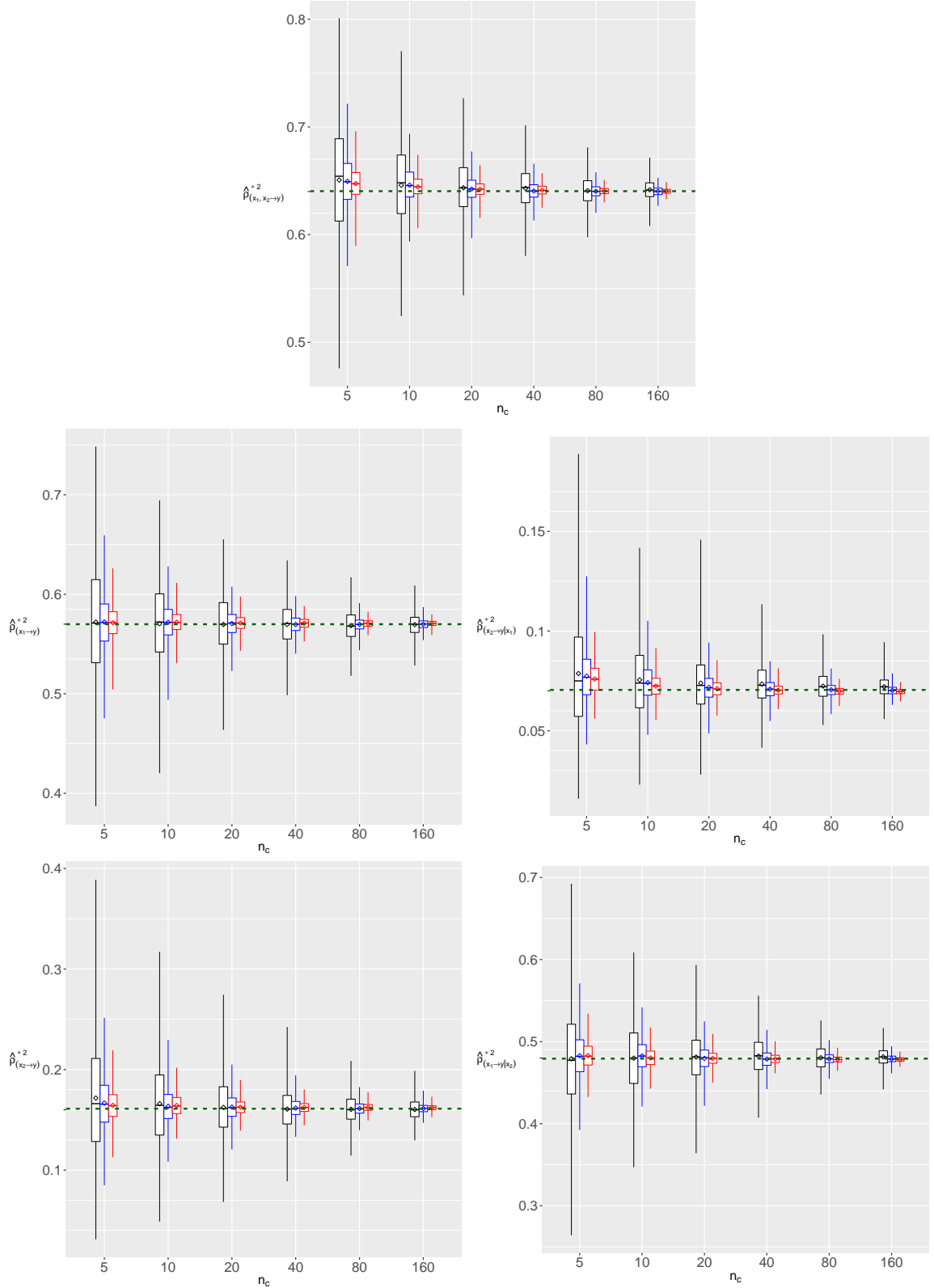


Fig. S16: Set IV-4 : Boxplots of $\hat{\rho}_{(x_1, x_2 \rightarrow y)}^{*2}$ (first row), $\hat{\rho}_{(x_1 \rightarrow y)}^{*2}$ (left in the second row), $\hat{\rho}_{(x_2 \rightarrow y|x_1)}^{*2}$ (right in the second row), $\hat{\rho}_{(x_2 \rightarrow y)}^{*2}$ (left in the third row), and $\hat{\rho}_{(x_1 \rightarrow y|x_2)}^{*2}$ (right in the third row) for the cell counts $n_c = (5, 10, 20, 40, 80, 160)$ under $3 \times 3 \times 3$ table (black colored boxplot), $5 \times 5 \times 5$ table (blue colored boxplot) and $7 \times 7 \times 7$ table (red colored boxplot)

S2.2 Simulation results

Table S3: Empirical convergence rates from the log-log plots of the RMSEs of $\hat{\rho}_{(X_1, X_2 \rightarrow Y)}^{2*}$, $\hat{\rho}_{(X_1 \rightarrow Y)}^{2*}$, $\hat{\rho}_{(X_2 \rightarrow Y|X_1)}^{2*}$, $\hat{\rho}_{(X_2 \rightarrow Y)}^{2*}$, and $\hat{\rho}_{(X_1 \rightarrow Y|X_2)}^{2*}$ and the total sample size n computed from 1000 simulated $3 \times 3 \times 3$, $5 \times 5 \times 5$ and $7 \times 7 \times 7$ tables

Parameter	$\hat{\rho}_{(X_1, X_2 \rightarrow Y)}^{2*}$	$\hat{\rho}_{(X_1 \rightarrow Y)}^{2*}$	$\hat{\rho}_{(X_2 \rightarrow Y X_1)}^{2*}$	$\hat{\rho}_{(X_2 \rightarrow Y)}^{2*}$	$\hat{\rho}_{(X_1 \rightarrow Y X_2)}^{2*}$
I	1	(-0.58, -0.63, -0.64)	(-1.02, -1, -1)	(-0.55, -0.6, -0.61)	(-0.52, -0.52, -0.5)
	2	(-0.55, -0.6, -0.63)	(-0.54, -0.52, -0.52)	(-0.53, -0.59, -0.62)	(-0.49, -0.51, -0.51)
	3	(-0.53, -0.55, -0.58)	(-0.52, -0.51, -0.51)	(-0.52, -0.56, -0.61)	(-0.5, -0.5, -0.52)
	4	(-0.52, -0.53, -0.55)	(-0.51, -0.5, -0.5)	(-0.51, -0.53, -0.56)	(-0.51, -0.52, -0.51)
II	1	(-0.56, -0.62, -0.65)	(-0.62, -0.6, -0.57)	(-0.54, -0.6, -0.63)	(-0.5, -0.51, -0.51)
	2	(-0.56, -0.59, -0.63)	(-0.51, -0.5, -0.52)	(-0.55, -0.61, -0.65)	(-0.5, -0.5, -0.51)
	3	(-0.53, -0.55, -0.58)	(-0.52, -0.5, -0.5)	(-0.58, -0.62, -0.67)	(-0.51, -0.5, -0.51)
	4	(-0.52, -0.54, -0.55)	(-0.5, -0.49, -0.49)	(-0.55, -0.6, -0.64)	(-0.52, -0.51, -0.49)
III	1	(-0.57, -0.62, -0.64)	(-0.54, -0.52, -0.52)	(-0.56, -0.61, -0.63)	(-0.5, -0.51, -0.5)
	2	(-0.56, -0.6, -0.63)	(-0.51, -0.5, -0.5)	(-0.62, -0.67, -0.72)	(-0.51, -0.51, -0.5)
	3	(-0.54, -0.55, -0.58)	(-0.5, -0.49, -0.5)	(-0.73, -0.79, -0.83)	(-0.51, -0.51, -0.5)
	4	(-0.5, -0.52, -0.56)	(-0.49, -0.49, -0.52)	(-0.95, -0.97, -0.99)	(-0.49, -0.51, -0.49)
IV	1	(-0.57, -0.6, -0.62)	(-0.53, -0.52, -0.5)	(-0.57, -0.63, -0.67)	(-0.52, -0.51, -0.5)
	2	(-0.55, -0.58, -0.6)	(-0.5, -0.49, -0.49)	(-0.77, -0.83, -0.88)	(-0.49, -0.5, -0.48)
	3	(-0.52, -0.55, -0.58)	(-0.51, -0.51, -0.51)	(-0.7, -0.81, -0.85)	(-0.52, -0.5, -0.51)
	4	(-0.5, -0.52, -0.53)	(-0.49, -0.49, -0.49)	(-0.51, -0.53, -0.55)	(-0.5, -0.51, -0.49)

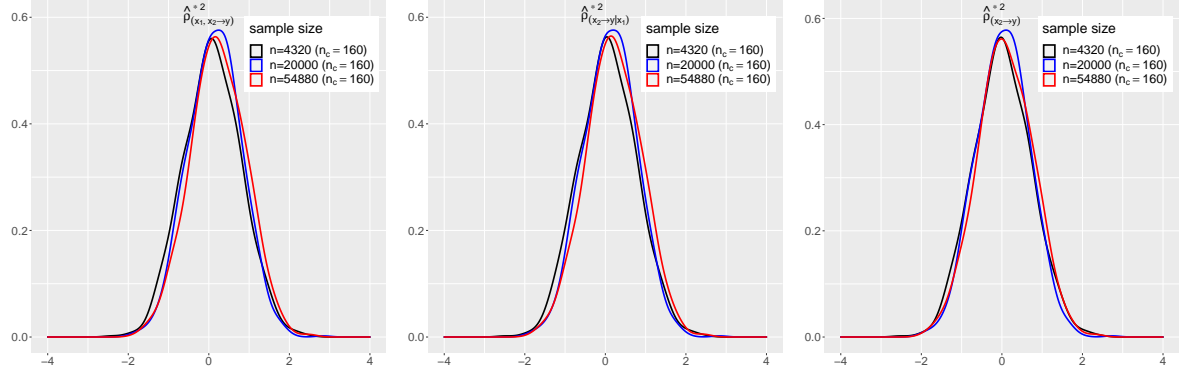


Fig. S17: Set I-1: Densities of the normalized estimates of $\hat{\rho}_{(x_1, x_2 \rightarrow y)}^{*2}$, $\hat{\rho}_{(x_2 \rightarrow y|x_1)}^{*2}$ and $\hat{\rho}_{(x_2 \rightarrow y)}^{*2}$ under $3 \times 3 \times 3$ table with $n=4320$ (black), $5 \times 5 \times 5$ table with $n=20000$ (blue) and $7 \times 7 \times 7$ table with $n=54880$ (red)

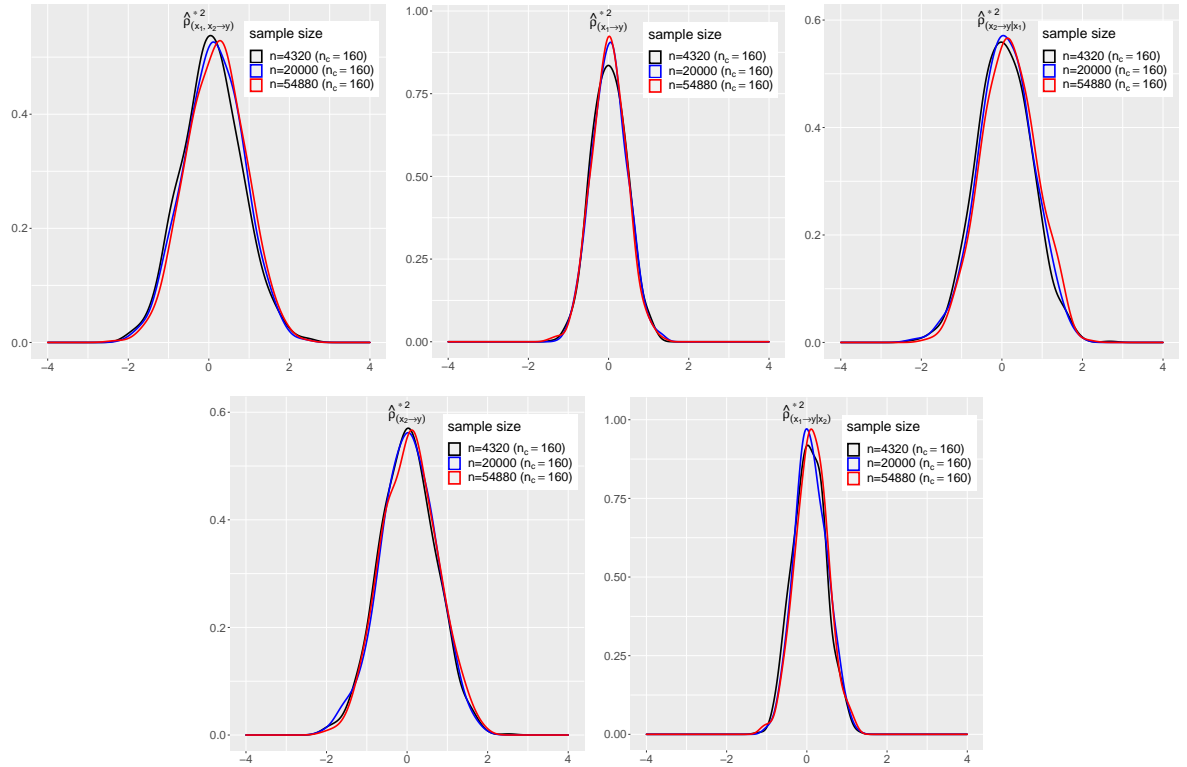


Fig. S18: Set I-2 : Densities of the normalized estimates of $\hat{\rho}_{(x_1, x_2 \rightarrow y)}^{*2}$, $\hat{\rho}_{(x_1 \rightarrow y)}^{*2}$, $\hat{\rho}_{(x_2 \rightarrow y|x_1)}^{*2}$, $\hat{\rho}_{(x_2 \rightarrow y)}^{*2}$, and $\hat{\rho}_{(x_1 \rightarrow y|x_2)}^{*2}$ under $3 \times 3 \times 3$ table with $n=4320$ (black), $5 \times 5 \times 5$ table with $n=20000$ (blue) and $7 \times 7 \times 7$ table with $n=54880$ (red)

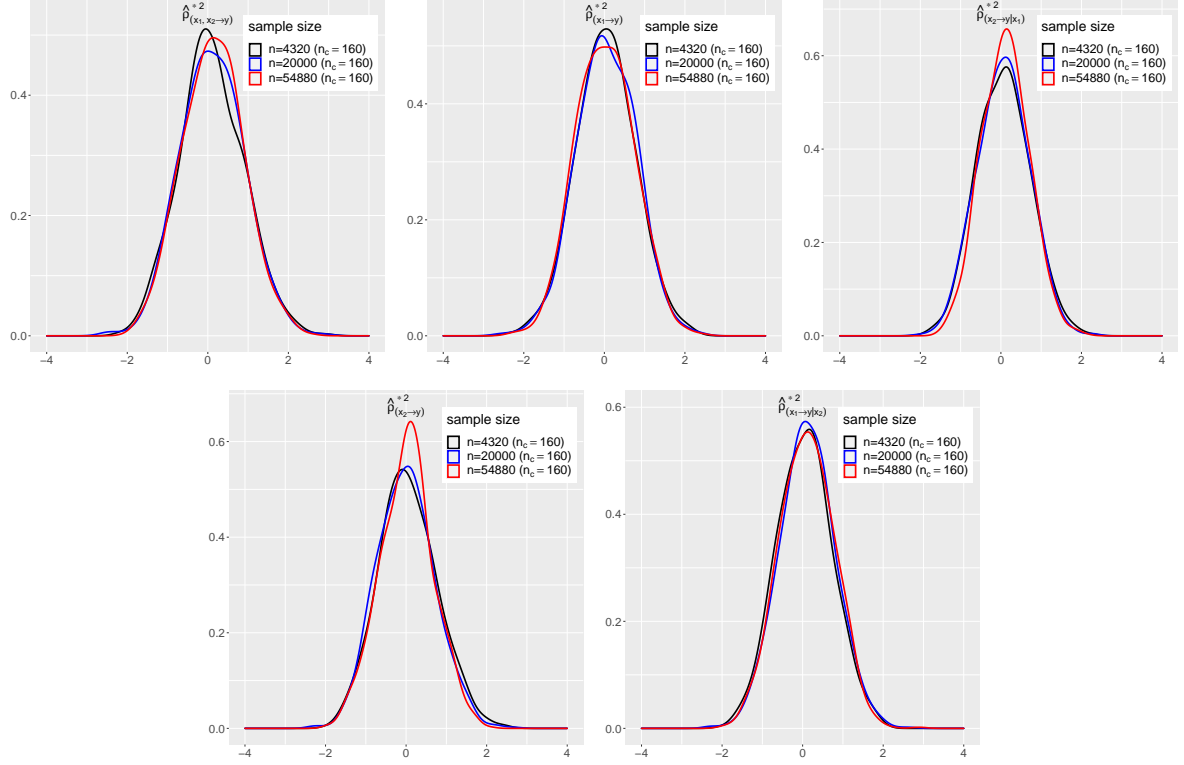


Fig. S19: Set I-3 : Densities of the normalized estimates of $\hat{\rho}_{(x_1, x_2 \rightarrow y)}^{2*}$, $\hat{\rho}_{(x_1 \rightarrow y)}^{2*}$, $\hat{\rho}_{(x_2 \rightarrow y|x_1)}^{2*}$, $\hat{\rho}_{(x_2 \rightarrow y)}^{2*}$ and $\hat{\rho}_{(x_1 \rightarrow y|x_2)}^{2*}$ under $3 \times 3 \times 3$ table with $n=4320$ (black), $5 \times 5 \times 5$ table with $n=20000$ (blue) and $7 \times 7 \times 7$ table with $n=54880$ (red)

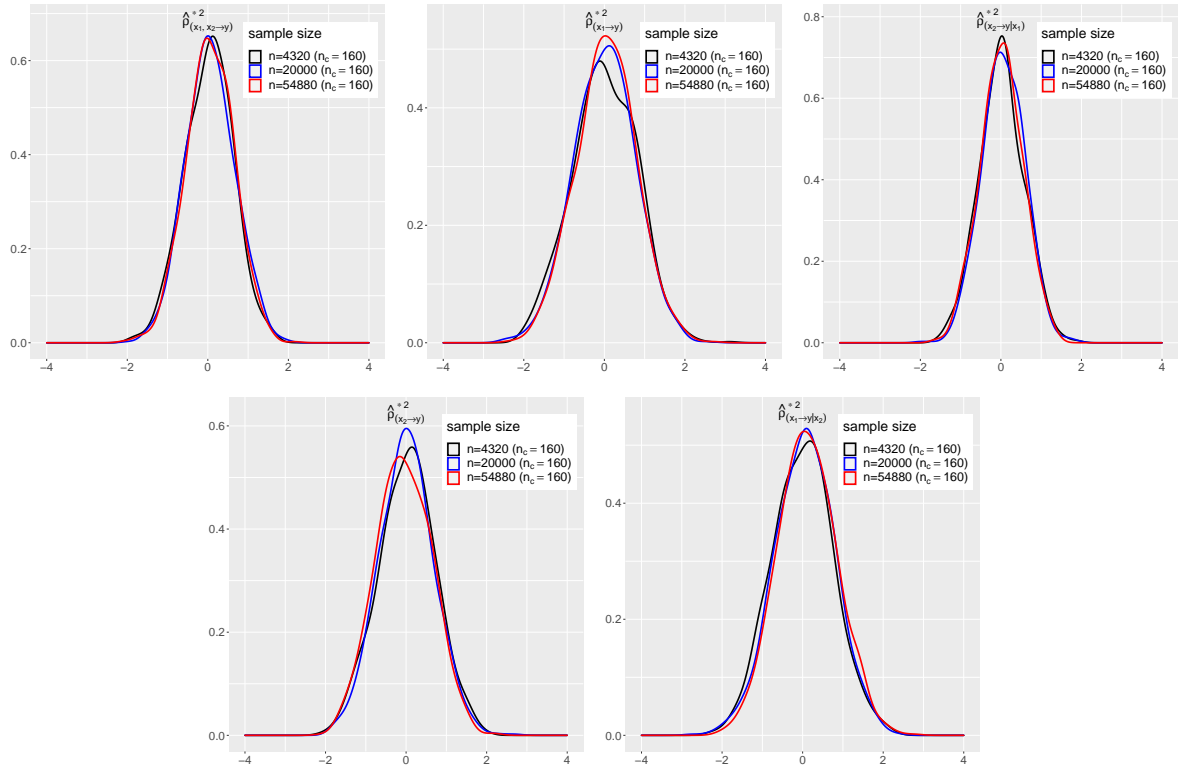


Fig. S20: Set I-4 : Densities of the normalized estimates of $\hat{\rho}_{(x_1, x_2 \rightarrow y)}^{2*}$, $\hat{\rho}_{(x_1 \rightarrow y)}^{2*}$, $\hat{\rho}_{(x_2 \rightarrow y|x_1)}^{2*}$, $\hat{\rho}_{(x_2 \rightarrow y)}^{2*}$ and $\hat{\rho}_{(x_1 \rightarrow y|x_2)}^{2*}$ under $3 \times 3 \times 3$ table with $n=4320$ (black), $5 \times 5 \times 5$ table with $n=20000$ (blue) and $7 \times 7 \times 7$ table with $n=54880$ (red)

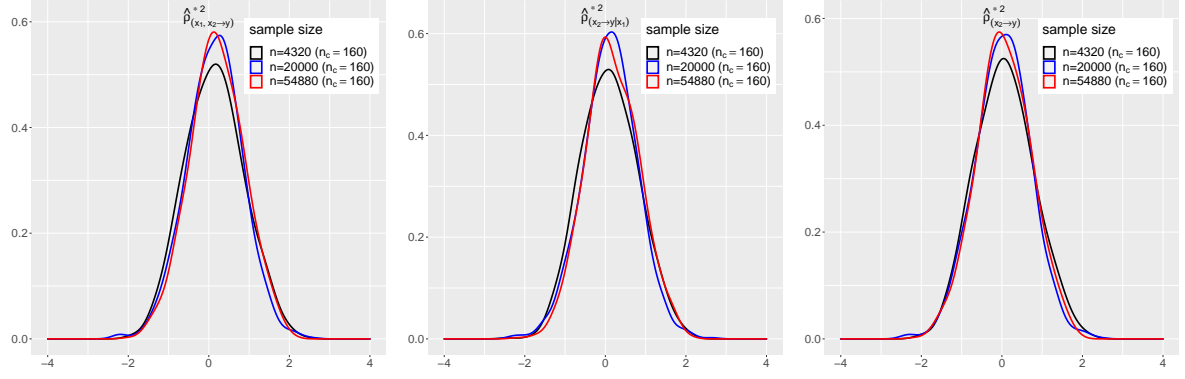


Fig. S21: Set II-1 : Densities of the normalized estimates of $\hat{\rho}^{2*}_{(X_1, X_2 \rightarrow Y)}$, $\hat{\rho}^{2*}_{(X_2 \rightarrow Y | X_1)}$, and $\hat{\rho}^{2*}_{(X_2 \rightarrow Y)}$ under $3 \times 3 \times 3$ table with $n=4320$ (black), $5 \times 5 \times 5$ table with $n=20000$ (blue) and $7 \times 7 \times 7$ table with $n=54880$ (red)

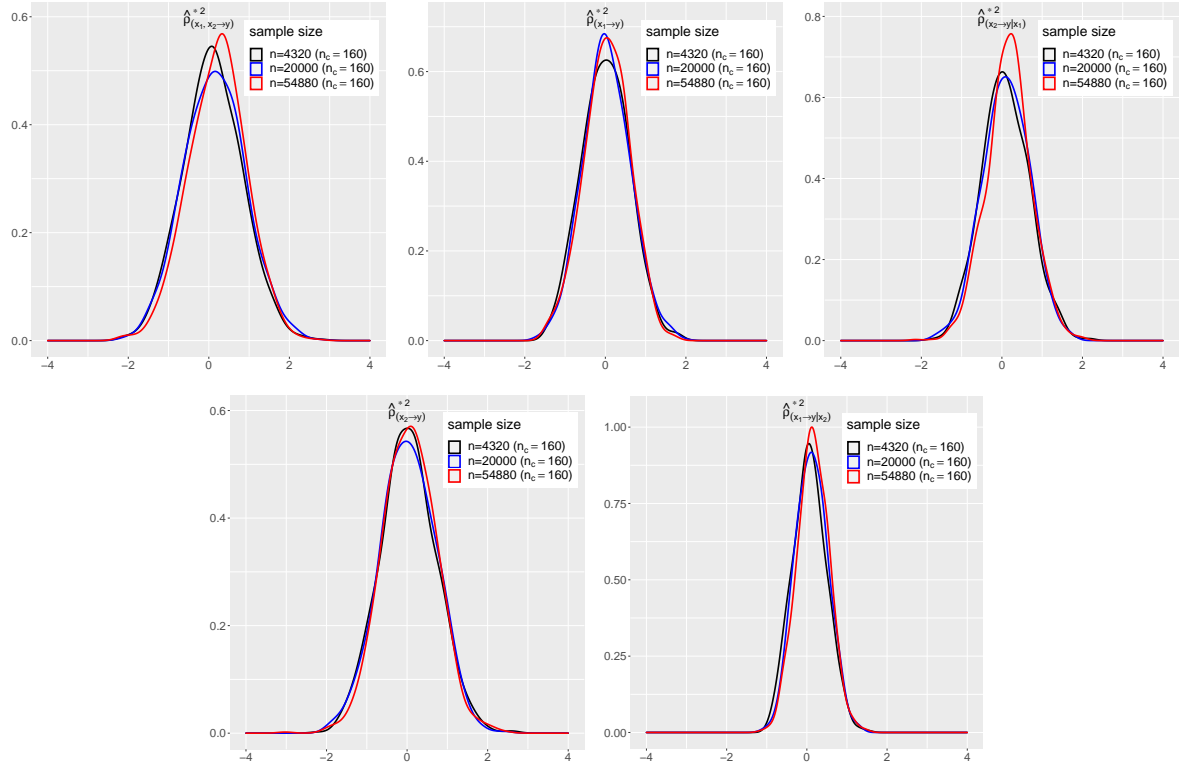


Fig. S22: Set II-2 : Densities of the normalized estimates of $\hat{\rho}^{2*}_{(X_1, X_2 \rightarrow Y)}$, $\hat{\rho}^{2*}_{(X_1 \rightarrow Y)}$, $\hat{\rho}^{2*}_{(X_2 \rightarrow Y | X_1)}$, $\hat{\rho}^{2*}_{(X_2 \rightarrow Y)}$, and $\hat{\rho}^{2*}_{(X_1 \rightarrow Y | X_2)}$ under $3 \times 3 \times 3$ table with $n=4320$ (black), $5 \times 5 \times 5$ table with $n=20000$ (blue) and $7 \times 7 \times 7$ table with $n=54880$ (red)

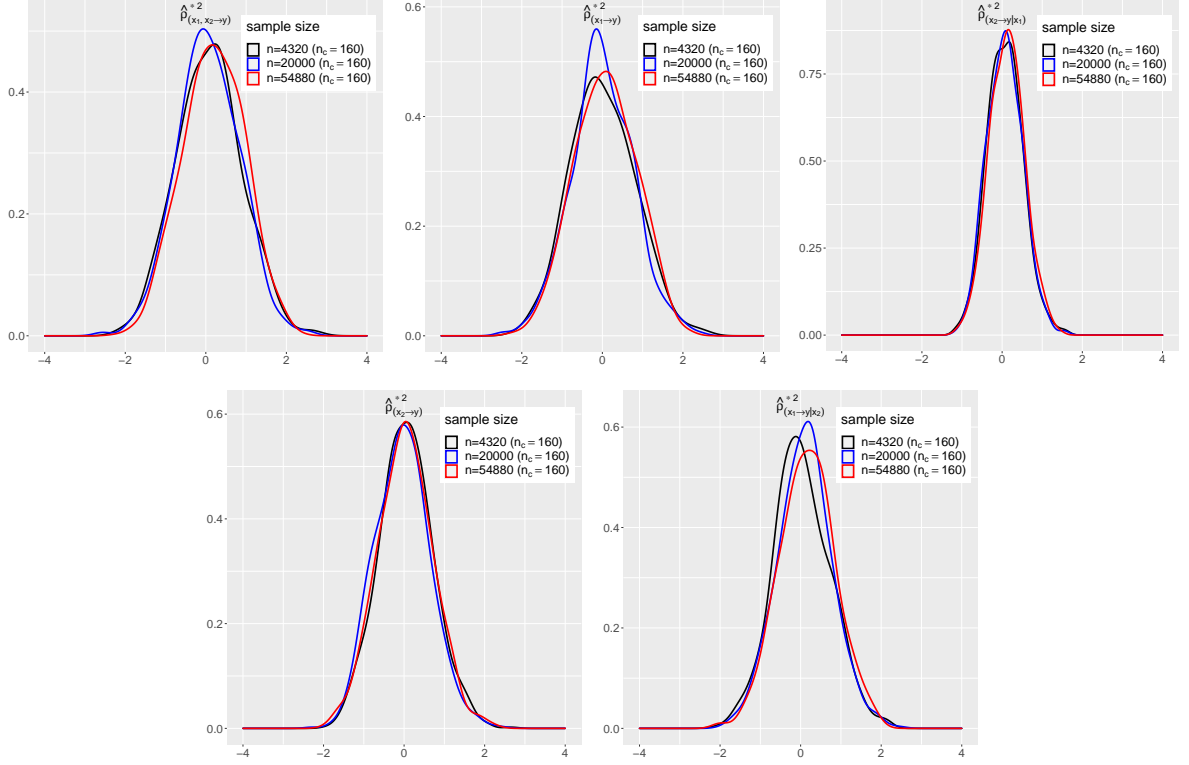


Fig. S23: Set II-3 : Densities of the normalized estimates of $\hat{\rho}^{2*}_{(X_1, X_2 \rightarrow Y)}$, $\hat{\rho}^{2*}_{(X_1 \rightarrow Y)}$, $\hat{\rho}^{2*}_{(X_2 \rightarrow Y|X_1)}$, $\hat{\rho}^{2*}_{(X_2 \rightarrow Y)}$, and $\hat{\rho}^{2*}_{(X_1 \rightarrow Y|X_2)}$ under $3 \times 3 \times 3$ table with $n=4320$ (black), $5 \times 5 \times 5$ table with $n=20000$ (blue) and $7 \times 7 \times 7$ table with $n=54880$ (red)

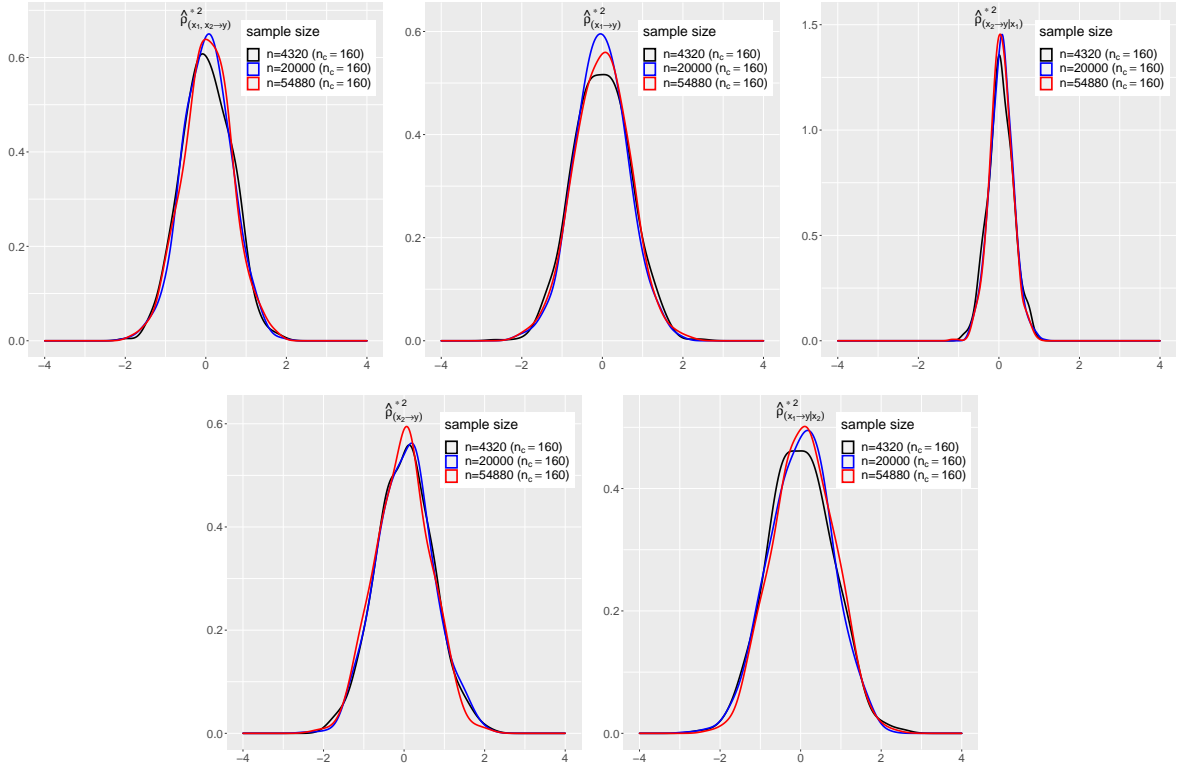


Fig. S24: Set II-4 : Densities of the normalized estimates of $\hat{\rho}^{2*}_{(X_1, X_2 \rightarrow Y)}$, $\hat{\rho}^{2*}_{(X_1 \rightarrow Y)}$, $\hat{\rho}^{2*}_{(X_2 \rightarrow Y|X_1)}$, $\hat{\rho}^{2*}_{(X_2 \rightarrow Y)}$, and $\hat{\rho}^{2*}_{(X_1 \rightarrow Y|X_2)}$ under $3 \times 3 \times 3$ table with $n=4320$ (black), $5 \times 5 \times 5$ table with $n=20000$ (blue) and $7 \times 7 \times 7$ table with $n=54880$ (red)

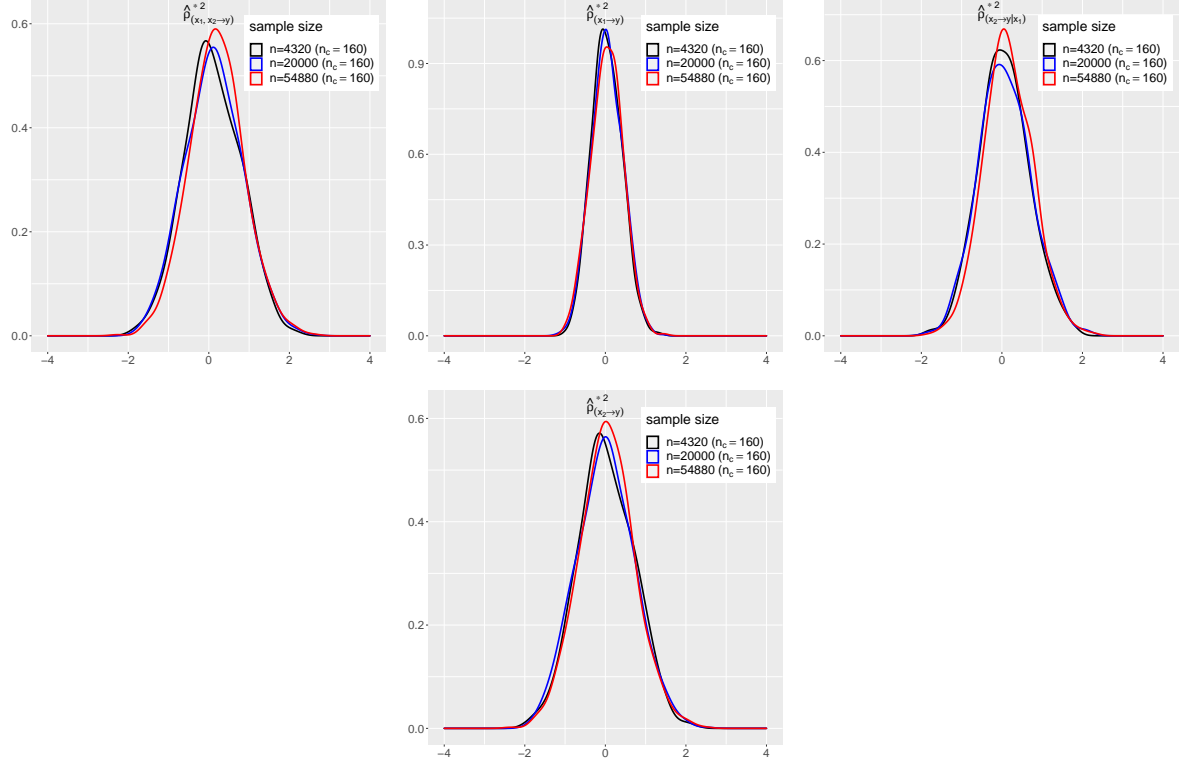


Fig. S25: Set III-1 : Densities of the normalized estimates of $\hat{\rho}_{(x_1, x_2 \rightarrow y)}^{*2}$, $\hat{\rho}_{(x_1 \rightarrow y)}^{*2}$, $\hat{\rho}_{(x_2 \rightarrow y|x_1)}^{*2}$, and $\hat{\rho}_{(x_2 \rightarrow y)}^{*2}$ under $3 \times 3 \times 3$ table with $n=4320$ (black), $5 \times 5 \times 5$ table with $n=20000$ (blue) and $7 \times 7 \times 7$ table with $n=54880$ (red)

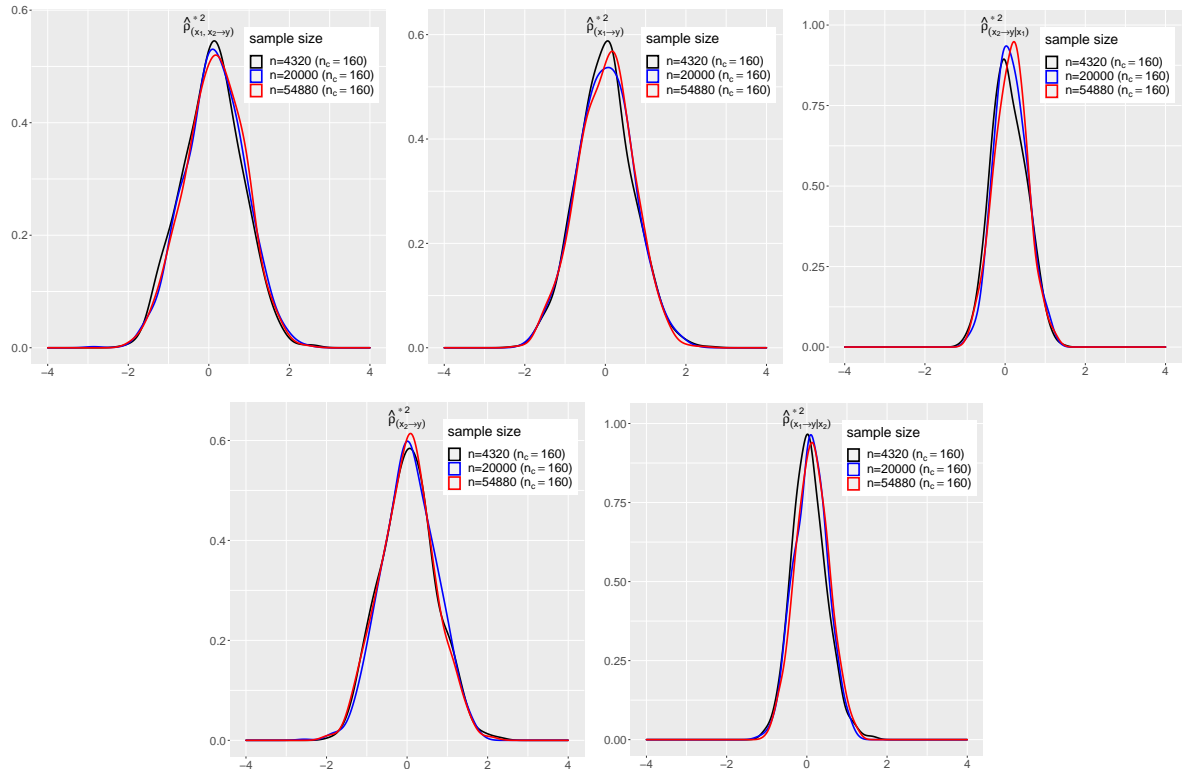


Fig. S26: Set III-2 : Densities of the normalized estimates of $\hat{\rho}_{(x_1, x_2 \rightarrow y)}^{*2}$, $\hat{\rho}_{(x_1 \rightarrow y)}^{*2}$, $\hat{\rho}_{(x_2 \rightarrow y|x_1)}^{*2}$, $\hat{\rho}_{(x_2 \rightarrow y)}^{*2}$, and $\hat{\rho}_{(x_1 \rightarrow y|x_2)}^{*2}$ under $3 \times 3 \times 3$ table with $n=4320$ (black), $5 \times 5 \times 5$ table with $n=20000$ (blue) and $7 \times 7 \times 7$ table with $n=54880$ (red)

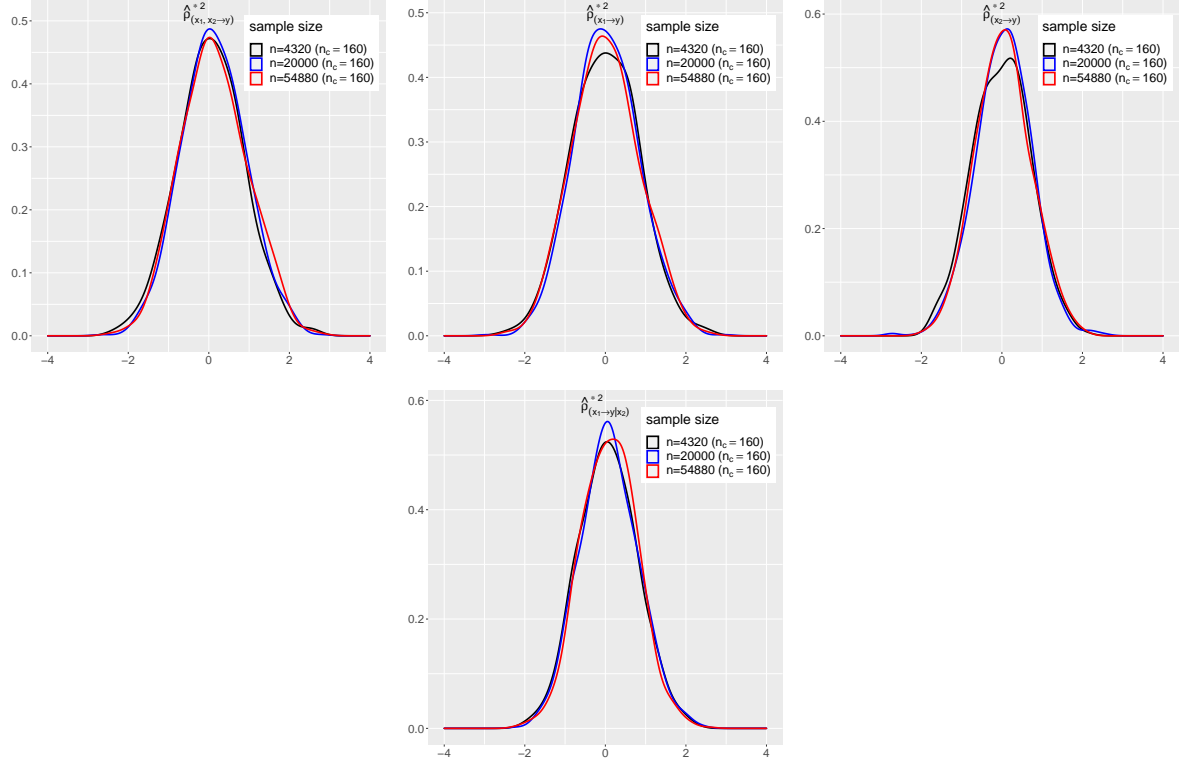


Fig. S27: Set III-3 : Densities of the normalized estimates of $\hat{\rho}_{(x_1, x_2 \rightarrow y)}^{*2}$, $\hat{\rho}_{(x_1 \rightarrow y)}^{*2}$, $\hat{\rho}_{(x_2 \rightarrow y)}^{*2}$, and $\hat{\rho}_{(x_1 \rightarrow y|x_2)}^{*2}$ under $3 \times 3 \times 3$ table with $n=4320$ (black), $5 \times 5 \times 5$ table with $n=20000$ (blue) and $7 \times 7 \times 7$ table with $n=54880$ (red)

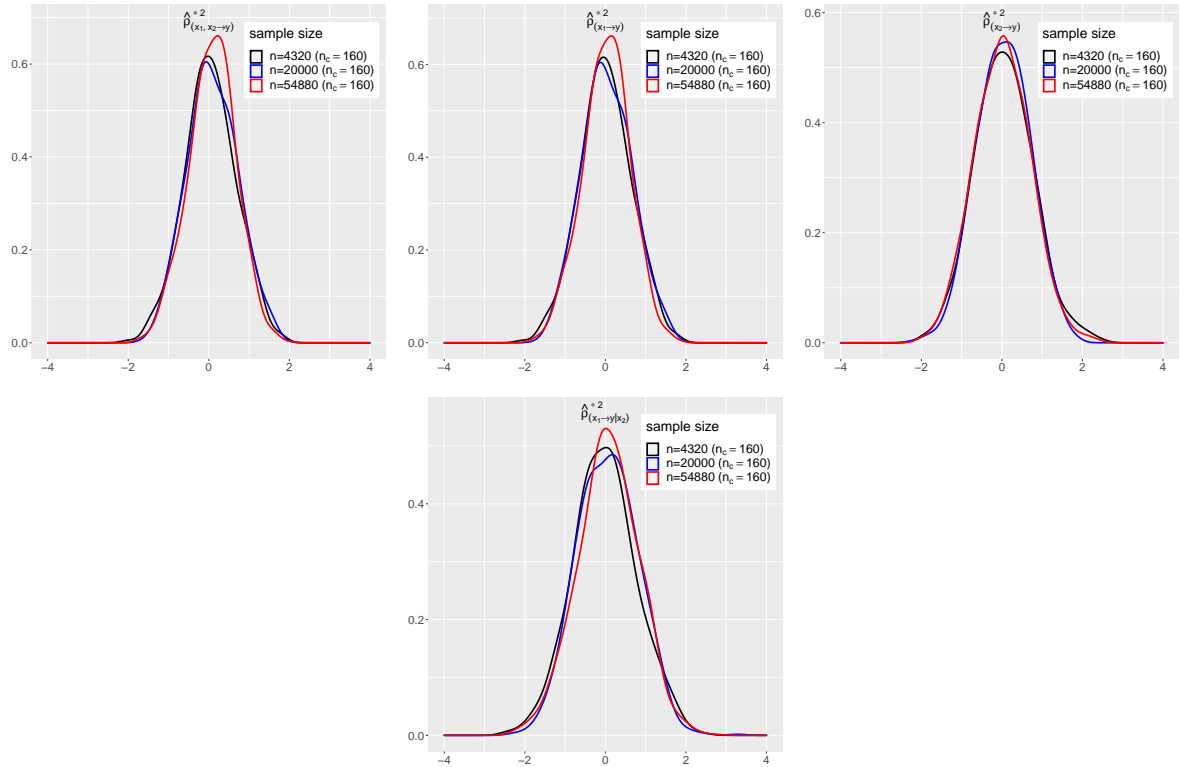


Fig. S28: Set III-4 : Densities of the normalized estimates of $\hat{\rho}_{(x_1, x_2 \rightarrow y)}^{*2}$, $\hat{\rho}_{(x_1 \rightarrow y)}^{*2}$, $\hat{\rho}_{(x_2 \rightarrow y)}^{*2}$ and $\hat{\rho}_{(x_1 \rightarrow y|x_2)}^{*2}$ under $3 \times 3 \times 3$ table with $n=4320$ (black), $5 \times 5 \times 5$ table with $n=20000$ (blue) and $7 \times 7 \times 7$ table with $n=54880$ (red)

S2.2 Simulation results

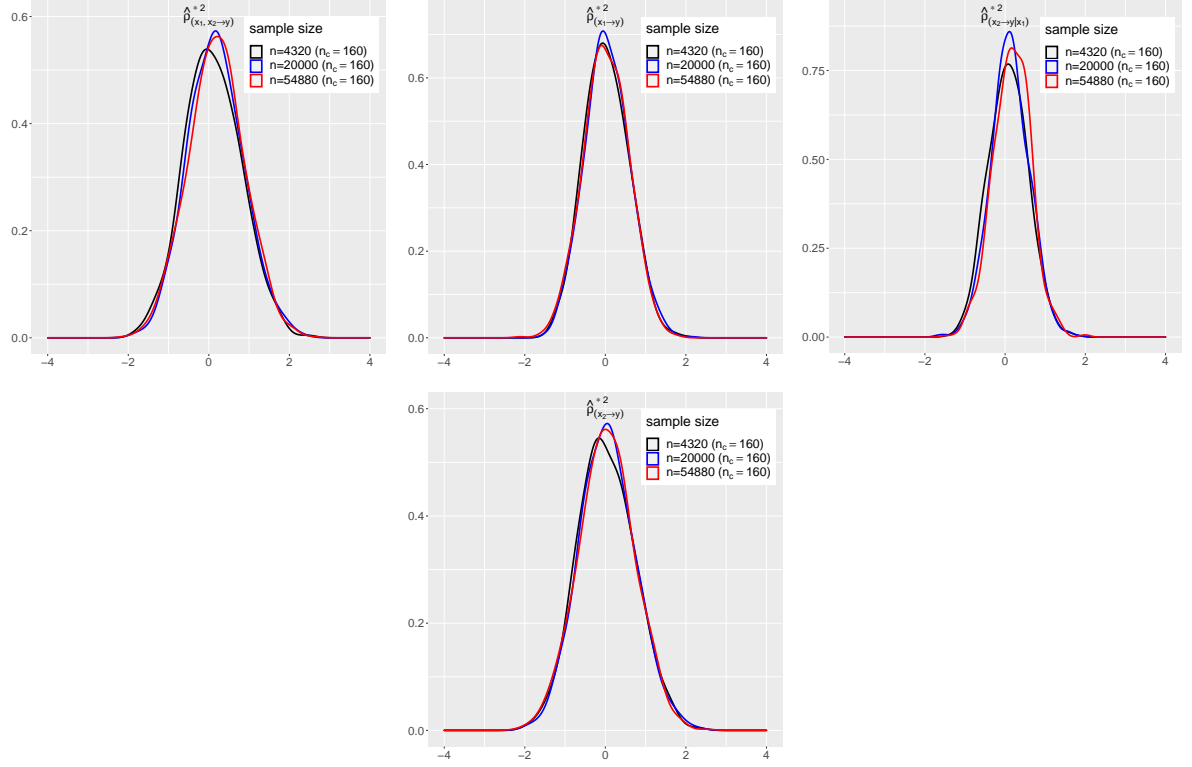


Fig. S29: Set IV-1 : Densities of the normalized estimates of $\hat{\rho}_{(x_1, x_2 \rightarrow y)}^{*2}$, $\hat{\rho}_{(x_1 \rightarrow y)}^{*2}$, $\hat{\rho}_{(x_2 \rightarrow y|x_1)}^{*2}$, and $\hat{\rho}_{(x_2 \rightarrow y)}^{*2}$ under $3 \times 3 \times 3$ table with $n=4320$ (black), $5 \times 5 \times 5$ table with $n=20000$ (blue) and $7 \times 7 \times 7$ table with $n=54880$ (red)

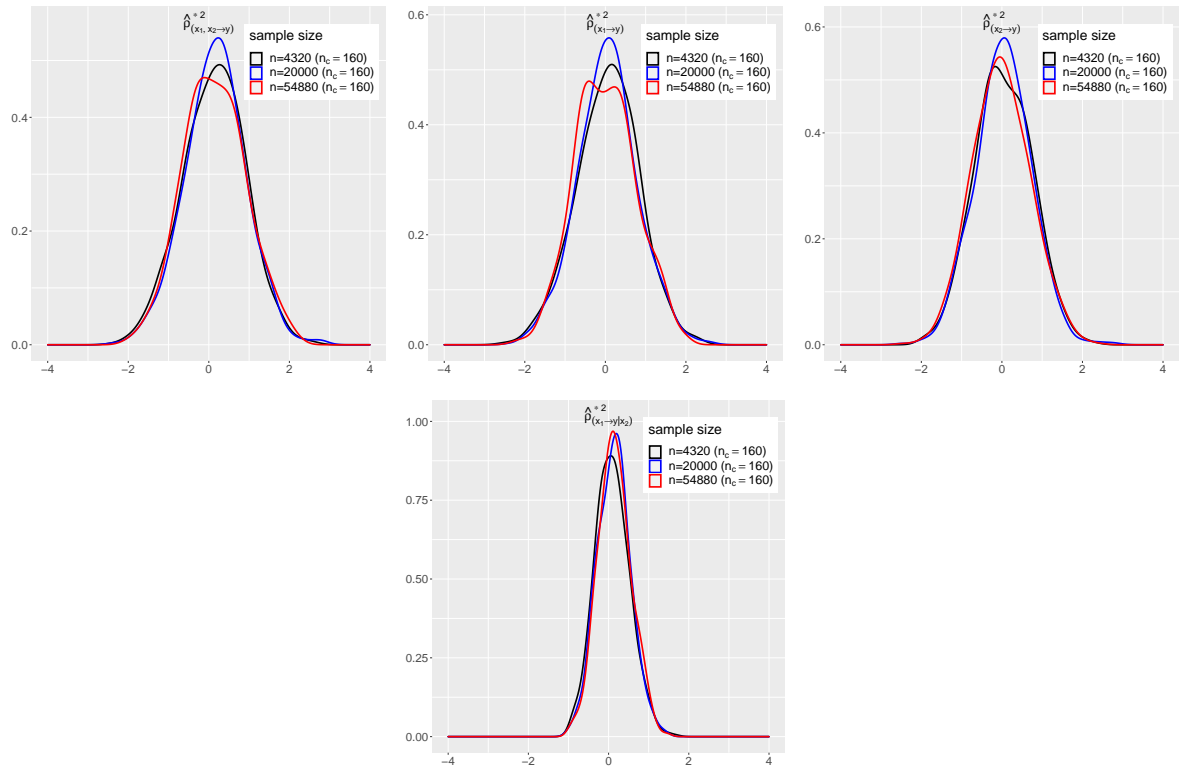


Fig. S30: Set IV-2 : Densities of the normalized estimates of $\hat{\rho}_{(x_1, x_2 \rightarrow y)}^{*2}$, $\hat{\rho}_{(x_1 \rightarrow y)}^{*2}$, $\hat{\rho}_{(x_2 \rightarrow y)}^{*2}$, and $\hat{\rho}_{(x_1 \rightarrow y|x_2)}^{*2}$ under $3 \times 3 \times 3$ table with $n=4320$ (black), $5 \times 5 \times 5$ table with $n=20000$ (blue) and $7 \times 7 \times 7$ table with $n=54880$ (red)

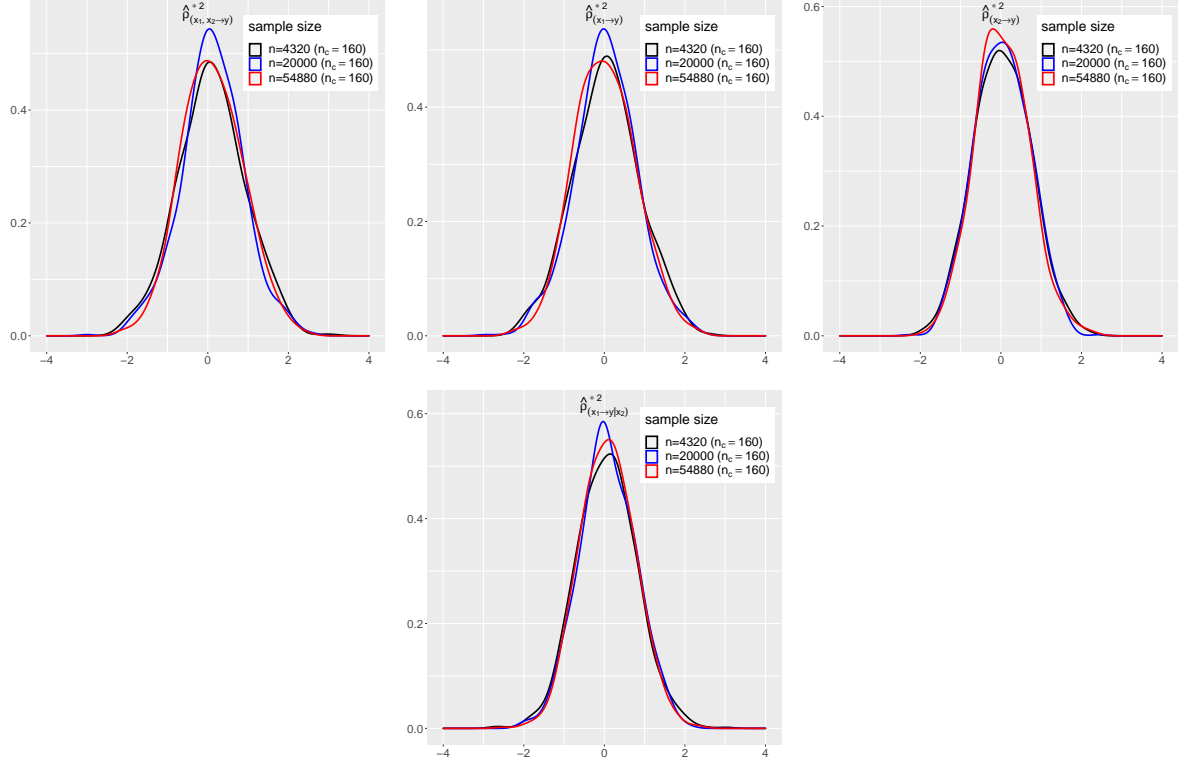


Fig. S31: Set IV-3 : Densities of the normalized estimates of $\hat{\rho}_{(x_1, x_2 \rightarrow y)}^{*2}$, $\hat{\rho}_{(x_1 \rightarrow y)}^{*2}$, $\hat{\rho}_{(x_2 \rightarrow y)}^{*2}$ and $\hat{\rho}_{(x_1 \rightarrow y|x_2)}^{*2}$ under $3 \times 3 \times 3$ table with $n=4320$ (black), $5 \times 5 \times 5$ table with $n=20000$ (blue) and $7 \times 7 \times 7$ table with $n=54880$ (red)

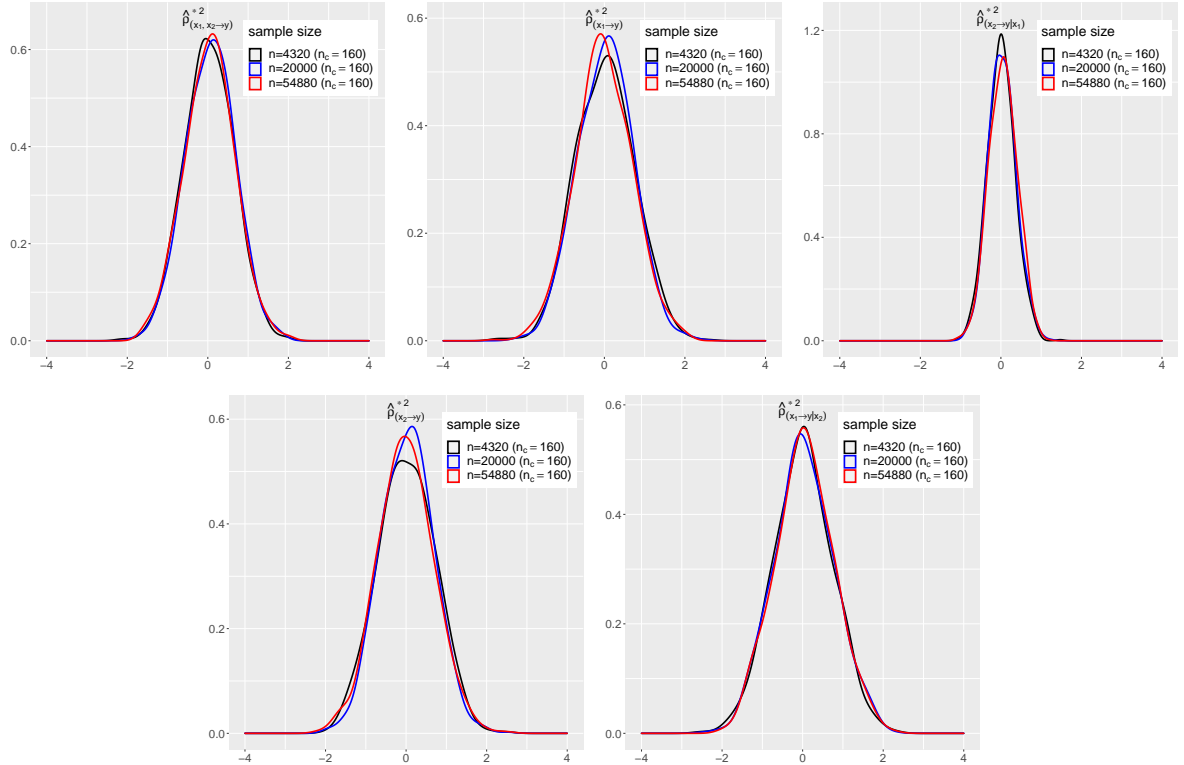


Fig. S32: Set IV-4 : Densities of the normalized estimates of $\hat{\rho}_{(x_1, x_2 \rightarrow y)}^{*2}$, $\hat{\rho}_{(x_1 \rightarrow y)}^{*2}$, $\hat{\rho}_{(x_2 \rightarrow y|x_1)}^{*2}$, $\hat{\rho}_{(x_2 \rightarrow y)}^{*2}$, and $\hat{\rho}_{(x_1 \rightarrow y|x_2)}^{*2}$ under $3 \times 3 \times 3$ table with $n=4320$ (black), $5 \times 5 \times 5$ table with $n=20000$ (blue) and $7 \times 7 \times 7$ table with $n=54880$ (red)

S2.2 Simulation results

Table S4: Empirical sizes of the permutation tests for $\rho_{(X_1, X_2 \rightarrow Y)}^{2*}$, $\rho_{(X_1 \rightarrow Y)}^{2*}$ and $\rho_{(X_1 \rightarrow Y|X_2)}^{2*}$ under the Case 0 in Table S2

Case 0	α	n_c	$\rho_{(X_1, X_2 \rightarrow Y)}^{2*}$			$\rho_{X_1 \rightarrow Y}^{2*}$			$\rho_{(X_1 \rightarrow Y X_2)}^{2*}$		
			$3 \times 3 \times 3$	$5 \times 5 \times 5$	$7 \times 7 \times 7$	$3 \times 3 \times 3$	$5 \times 5 \times 5$	$7 \times 7 \times 7$	$3 \times 3 \times 3$	$5 \times 5 \times 5$	$7 \times 7 \times 7$
0.05		5	0.053	0.046	0.059	0.038	0.052	0.065	0.054	0.050	0.055
		10	0.046	0.047	0.055	0.048	0.053	0.044	0.052	0.047	0.036
		20	0.043	0.052	0.046	0.039	0.058	0.052	0.048	0.047	0.049
		40	0.062	0.051	0.047	0.063	0.033	0.046	0.048	0.049	0.053
		80	0.043	0.055	0.042	0.056	0.046	0.046	0.054	0.048	0.049
		160	0.064	0.057	0.062	0.057	0.053	0.059	0.060	0.054	0.060
0.01		5	0.007	0.014	0.007	0.003	0.011	0.010	0.008	0.008	0.012
		10	0.009	0.011	0.014	0.018	0.013	0.007	0.013	0.012	0.004
		20	0.012	0.009	0.006	0.002	0.007	0.015	0.013	0.010	0.006
		40	0.011	0.009	0.009	0.012	0.008	0.007	0.016	0.012	0.008
		80	0.007	0.012	0.006	0.007	0.006	0.008	0.008	0.006	0.009
		160	0.013	0.012	0.013	0.010	0.009	0.009	0.012	0.008	0.011

Table S5: Empirical sizes for $\rho_{(X_1 \rightarrow Y)}^{2*}$ and $\rho_{(X_1 \rightarrow Y|X_2)}^{2*}$, and empirical power for $\rho_{(X_1, X_2 \rightarrow Y)}^{2*}$ under the Case 1 in Table S2

Case 1	α	n_c	$\rho_{(X_1, X_2 \rightarrow Y)}^{2*}$			$\rho_{X_1 \rightarrow Y}^{2*}$			$\rho_{(X_1 \rightarrow Y X_2)}^{2*}$		
			$3 \times 3 \times 3$	$5 \times 5 \times 5$	$7 \times 7 \times 7$	$3 \times 3 \times 3$	$5 \times 5 \times 5$	$7 \times 7 \times 7$	$3 \times 3 \times 3$	$5 \times 5 \times 5$	$7 \times 7 \times 7$
0.05		5	0.934	1	1	0.047	0.057	0.050	0.043	0.050	0.049
		10	1	1	1	0.063	0.056	0.047	0.049	0.065	0.061
		20	1	1	1	0.040	0.052	0.047	0.039	0.046	0.050
		40	1	1	1	0.050	0.044	0.053	0.048	0.039	0.049
		80	1	1	1	0.063	0.044	0.045	0.057	0.046	0.046
		160	1	1	1	0.059	0.041	0.057	0.054	0.055	0.058
0.01		5	0.842	1	1	0.005	0.008	0.010	0.008	0.012	0.011
		10	0.999	1	1	0.010	0.011	0.011	0.007	0.011	0.009
		20	1	1	1	0.008	0.009	0.010	0.014	0.014	0.012
		40	1	1	1	0.010	0.009	0.009	0.007	0.007	0.010
		80	1	1	1	0.011	0.009	0.007	0.017	0.008	0.010
		160	1	1	1	0.011	0.009	0.013	0.017	0.007	0.009

Table S6: Empirical powers of the permutation tests for $\rho_{(X_1, X_2 \rightarrow Y)}^{2*}$, $\rho_{(X_1 \rightarrow Y)}^{2*}$ and $\rho_{(X_1 \rightarrow Y|X_2)}^{2*}$ under the Case 2 in Table S2

[illegible]

Table S7: Empirical powers of the permutation tests for $\rho_{(X_1, X_2 \rightarrow Y)}^{2*}$, $\rho_{(X_1 \rightarrow Y)}^{2*}$ and $\rho_{(X_1 \rightarrow Y|X_2)}^{2*}$ under the Case 3 in Table S2

[illegible]

Table S8: Empirical powers of the permutation tests for $\rho_{(X_1, X_2 \rightarrow Y)}^{2*}$, $\rho_{(X_1 \rightarrow Y)}^{2*}$ and $\rho_{(X_1 \rightarrow Y|X_2)}^{2*}$ under the Case 4 in Table S2

[illegible]

Table S9: Empirical powers of the permutation tests for $\rho_{(X_1, X_2 \rightarrow Y)}^{2*}$, $\rho_{(X_1 \rightarrow Y)}^{2*}$ and $\rho_{(X_1 \rightarrow Y|X_2)}^{2*}$ under the Case 5 in Table S2

[illegible]

References

- [1] A. Agresti, M. Yang, An empirical investigation of some effects of sparseness in contingency tables, *Computational Statistics & Data Analysis* 5 (1987) 9–21.
- [2] A. Barbiero, P. Ferrari, GenOrd: Simulation of Discrete Random Variables with Given Correlation Matrix and Marginal Distributions, 2015. R package version 1.4.0.
- [3] P. A. Ferrari, A. Barbiero, Simulating ordinal data, *Multivariate Behavioral Research* 47 (2012) 566–589.